Report 1603

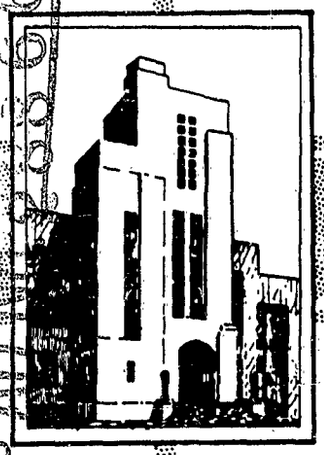

DEPARTMENT OF THE NAVY

DAVID TAYLOR MODEL BASIN

HYDROMECHANICS

AERODYNAMICS

STRUCTURAL MECHANICS

APPLIED MATHEMATICS

THRUST DEDUCTION DUE TO A PROPELLER BEHIND A HYDROFOIL

by

John L. Beveridge

HYDROMECHANICS LABORATORY
RESEARCH AND DEVELOPMENT REPORT

October 1962 Report 1603

TABLE OF CONTENTS

LIST OF FIGURES

LIST OF TABLES

NOTATION

A	Propeller-disk area
C_D	Total augmented-resistance coefficient
C_{D_1}	Mean augmented-resistance coefficient
C_{d_o}	Section profile-drag coefficient
C_f	Frictional-resistance coefficient
C_L	Lift coefficient
C_T	Propeller thrust-loading coefficient $\frac{T}{\frac{1}{2}\rho A V_a^2}$
C_t	Total-resistance coefficient
c	Chord or section length
D	Total augmented-foil resistance (due to T)
D_1	Mean augmented-foil resistance (due to $\overline{T}$)
d	Propeller diameter
$F_j = Q, L$, etc.	Force
J	Propeller-speed coefficient
L	Foil span measured from top of water tunnel jet to the free end of the foil
l	Foil span measured from axis of water tunnel (propeller axis) to the free end of the foil
n	Propeller frequency of revolution (rps)
n'	Propeller equivalent (rps)
Q	Output of a point source
q	Output of a line source
q_o	Stagnation pressure $\frac{1}{2}\rho V^2$
q^*	Output of a surface source
R	Resistance or propeller-tip radius
R_n	Reynolds number
r	Local radius or radius vector
S	Wetted surface
T	Propeller-fluctuating total thrust
$\overline{T}$	Propeller average thrust
t	Total thrust-deduction coefficient (also section thickness)
t_1	Mean thrust-deduction coefficient

V	Transport velocity or undisturbed velocity
V_a	Propeller speed of advance = $V(1-W)$
W	Taylor or effective wake fraction
W_L	Longitudinal wake fraction
W_P	Potential wake fraction
W_t	Tangential wake fraction
x	Radius fraction r/R or a length
α	Angle of attack
α_{Lo}	Angle of zero lift
β	Propeller-advance angle
ζ	Wake half-width
ζ'	Vertical distance from wake centerline
η	Loss in dynamic pressure at wake center as a fraction of q_0
η'	Loss in dynamic pressure as a fraction of q_0
θ'	Propeller-blade position
ν	Kinematic viscosity
ξ	Distance behind foil trailing edge in chords
ρ	Mass density
ω	Angular velocity = $2\pi n$

ABSTRACT

A method which is based on Lagally's theorem is presented for computing the resistance augmentation, or thrust deduction, for submerged hydrofoil-propeller arrangements. The effect on the magnitude of thrust deduction of foil lift, propeller load, foil span, foil flap angle, and propeller-foil spacing was investigated. Computed examples and experimental thrust-deduction results for several hypothetical arrangements showed good agreement.

INTRODUCTION

In recent years, a great deal of theoretical and experimental work has been performed in the field of propulsion interaction.[1-6] In particular, considerable emphasis has been placed on propulsion interaction effects as associated with submerged bodies of revolution with application to submarine powering. As a result, important data and criteria are now available for determining the coefficients of interaction, i.e., wake fraction and thrust deduction, for various hull and propeller arrangements. In contrast, this report deals with propulsion interaction phenomena for hydrofoil and propeller combinations with application to powering of high-speed, hydrofoil-supported craft. Although the investigations already mentioned have used singularity systems which are similar to those used herein, an application leading to design criteria for hydrofoils has not been done previously. The present work differs from solutions for a body of revolution principally in the detail consideration of the singularities which represent the propeller. The propeller singularities are based on total fluctuating thrust as obtained from quasi-steady propeller theory using empirical viscous-wake data.

The study reported herein proposes to establish an analytical method for estimating the resistance augmentation due to propeller action on submerged nonoscillating hydrofoil configurations. An application of Lagally's theorem is used to find the augmented resistance of a hydrofoil; this application gives solutions for (1) the effect of various parameters on the augmented resistance of hydrofoils and (2) propeller performance in a nonuniform wake.

To verify the analytical study, experiments were made on various propeller-hydrofoil arrangements in the 24-in. water tunnel at the David Taylor Model Basin. The scope of the experimental work included:

1. Determination of the augmented resistance of a lifting foil for conditions which represent, with and without nacelle, infinite span and semi-infinite span.

2. Investigation of the effect of variations in propeller load, propeller spacing, and foil angle-of-attack on the augmented resistance of the foil.

In this report, the theoretical equations which provide a solution of the interaction force are discussed first, and then necessary expressions and data for the wake of the foil

---

[1] References are listed on page 36.

and total propeller thrust are derived. Finally, the computational results and the experimental phases of the work are presented and compared.

This work was accomplished with the support of the Bureau of Ships Fundamental Hydromechanics Research Program.

STATEMENT OF PROBLEM

In potential flow, mathematical singularities which represent solid bodies or boundaries are widely used. The Lagally steady-motion formula[5,7] relates the force experienced by a source of given output (or a sink of given input) in an arbitrarily formed flow to the velocity which the surrounding flow, undisturbed by the source, possesses at the location of the source. Lagally's steady-motion theorem can be used to obtain a solution of the quasi-steady interaction force (thrust deduction) for a propeller-hydrofoil system. The thrust-deduction problem is analogous to the familiar problem of finding the forces between two bodies in a flow field. A force arises from the mutual influence of the foil on the propeller and the propeller on the foil. Simply stated, a foil affects propeller performance through its wake, and a foil (from the point of view of resistance) is affected by the induced velocity field of a propeller.

Lagally's theorem provides a means of circumventing the detail of integrating pressures over the foil surface to obtain the thrust-deduction force. Since the interaction force is to be obtained directly from relations between singularities, the main problem is to find appropriate generating singularities for a hydrofoil and a propeller. Essential parts of the problem are determination of the disturbing wake velocities due to a foil situated in a uniform potential flow and determination of propeller-fluctuating thrust. Specifically, these essential parts enter into the solution of the interaction or thrust-deduction force, using the Lagally theorem, by providing the required foil-disturbance velocity and propeller-sink input. Propeller-thrust fluctuations were estimated by calculating quasi-steady propeller forces. Inasmuch as propeller-fluctuating thrust is caused mostly by the nonuniformities (as seen by the propeller) in the wake of the hydrofoil and the viscous part is large, expressions for the viscous wake must also be obtained. For this purpose, NACA empirical wake data were used as a basis for obtaining viscous-wake distributions.

The principal *assumptions* and *limitations* that are involved in the analysis and treatment of the problem are summarized as follows:

1. Interference effects which involve changes in boundary conditions and lead to iterations are not considered.

2. The effects of various singularities can be combined. Exact linear superposition of flows is, of course, limited to those flows which satisfy the Laplace equation. It is assumed that the effect of the propeller on the foil is mainly potential in origin, whereas the effect of the foil on the propeller is essentially viscous in origin. The effect on the propeller is treated, however, as a potential problem through the use of the total wake at the propeller.

3. A distribution of viscous wake behind a hydrofoil is obtained by assuming that the static pressure is zero within the wake. This assumption seems reasonable since the pressure decays rapidly downstream behind a well-streamlined foil.

4. It is assumed that a propeller can be simulated by a distributed sink disk of circumferentially variable strength. This is an adequate representation for calculating thrust deduction (for stern propellers) since physically the suction field ahead of a propeller is important and the velocity field ahead of a propeller has no vorticity.

5. The assumption is made that quasi-steady propeller forces can be used to estimate propeller-thrust fluctuations due to a nonuniform wake distribution.

ANALYSIS

EXPRESSIONS FOR THE FOIL-RESISTANCE AUGMENTATION

A body in a fluid may experience a lift force normal to the flow direction. The force assuming potential flow is given by the well-known Kutta-Joukowsky relation

$$F_L = \rho V \Gamma$$

where F_L is the lift force per unit length,

ρ is the mass density of the fluid,

V is the undisturbed velocity, and

Γ is the circulation around the body.

Vortex distributions can be used in combination with other flows to represent solid bodies. Flows about hydrofoils with circulation can be generated in this way.

Lagally's steady-motion equation[5]

$$F_Q = -\rho Q_1 \frac{Q_2}{4\pi r^2} \qquad [1]$$

connects the force F_Q experienced by a source at some point in the flow field with the output Q_1 and the flow velocity $\frac{Q_2}{4\pi r^2}$ at the location of the source Q_1, where r is the distance from a source Q_2 to a source Q_1. When the single sources of Equation [1] are replaced by line- and surface-source distributions, the interaction force (drag augment) of a propeller-hydrofoil system is obtained by using the disturbing velocities

$$W_P V = \int_x \frac{q(x)\,dx}{4\pi r^2}$$

from the foil acting at the surface-sink distribution (propeller) of input

$$\int_A q^*(A)\,dA$$

W_P is the absolute nondimensional perturbation velocity which represents the disturbance of the velocity V caused by the foil in a potential flow. This approach is a matter of convenience inasmuch as the same force would arise by considering the propeller-induced velocity field as acting at the foil. To be equivalent, however, it should be noted that only the potential part of the foil velocity is used at the propeller. The arrangement and coordinates of the propeller-hydrofoil system are shown in Figure 1.

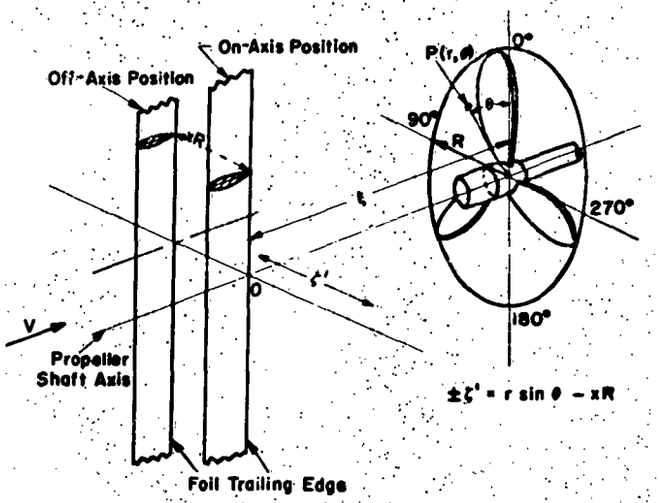

Figure 1 – Arrangement of Propeller and Hydrofoil System

It is desired to find expressions for and to compute values of the total augmented-drag coefficient C_D and the mean-drag coefficient C_{D_1}. Equation [1] can be written in terms of the foil-disturbing potential velocities $W_P V$ at the propeller disk and a distributed surface sink of total strength $\left(\frac{q^*}{4\pi}\right)$.

Dimensionally, the relation is

$$D = \rho V \int_0^{2\pi} \int_{\text{hub}}^{R} q^* W_P r\,dr\,d\theta \qquad [2]$$

and the total augmented drag is given as a coefficient by writing Equation [2] in the following nondimensional form:

$$C_D = \frac{D}{\rho V^2 (1-W) R^2} = \int_0^{2\pi} \int_{xh}^{x=1} \frac{q^*}{V_a} W_p x dx d\theta \qquad [3]$$

The total surface-sink input q^* is related to propeller total thrust-loading coefficient from momentum considerations by

$$q^* = [-1 + (1+C_T)^{1/2}] V_a \qquad [4]$$

Since the propeller thrust varies with propeller-blade position, the sink input q^* also varies circumferentially. Similar to Equation [4], a mean surface-sink input q_1^* is related to propeller mean thrust with

$$q_1^* = [-1 + (1+\overline{C}_T)^{1/2}] V_a \qquad [4a]$$

where $\overline{C}_T$ is the mean thrust-loading coefficient, and a mean augmented-drag coefficient is given by

$$C_{D_1} = \frac{D_1}{\rho V^2 (1-W) R^2} = \frac{q_1^*}{V_a} \int_0^{2\pi} \int_{xh}^{1} W_p x dx d\theta \qquad [5]$$

Interaction force has been discussed as an augmented drag D or augmented-drag coefficient C_D. The expression $D = T - R$ (where T is propeller-fluctuating total thrust and R is foil resistance without a propeller) is variously called the thrust-deduction force or resistance augmentation. The ratio of the difference D to propeller average thrust $\overline{T}$ is known as the thrust-deduction coefficient t. The thrust-deduction coefficient can be related to the augmented-drag coefficient by

$$t = \frac{D}{\overline{T}} = \frac{2C_D}{\overline{C}_T \pi (1-W)}$$

$$t_1 = \frac{D_1}{\overline{T}} = \frac{2C_{D_1}}{\overline{C}_T \pi (1-W)}$$

EXPRESSIONS FOR THE VISCOUS WAKE OF HYDROFOILS

The National Advisory Committee for Aeronautics has made theoretical studies and detailed measurements of the wake behind various airfoils and has derived empirical equations from some of these data.[8,9] Moreover, present knowledge concerning free turbulent shear flows has established the relevant wake characteristics, e.g., the total pressure loss

is a maximum in the center of the wake and decreases to zero at the wake edge. Turbulent mixing causes the total pressure loss to decrease with distance downstream and a consequent increase in wake width. Some pertinent empirical equations, which resulted from the subject method of analysis, follow.

Wake width and maximum loss of dynamic pressure in the wake is given in terms of profile-drag coefficient and distance behind the trailing edge of the foil. The wake half-width is

$$\zeta = 0.68\, C_{d_o}^{1/2}\, (\xi + 0.15)^{1/2} \qquad [6]$$

where ζ is the wake half-width in chords,

ξ is the distance behind the foil trailing edge in chords, and

C_{d_o} is the section profile-drag coefficient.

The maximum loss of dynamic pressure is

$$\eta = \frac{2.42\, C_{d_o}^{1/2}}{\xi + 0.3}\,, \quad \xi \leq 3 \qquad [7]$$

where η is the loss in dynamic pressure at the wake center as a fraction of q_o. A distribution of dynamic pressure within the wake is given as a cosine squared function

$$\frac{\eta'}{\eta} = \cos^2\left(\frac{\pi}{2}\,\frac{\zeta'}{\zeta}\right) \qquad [8]$$

It is assumed that, within the wake, the static pressure is zero and, at the edge of the wake, the velocity is everwhere, freestream velocity V. Based on the foregoing, the wake factor is estimated from the relation

$$(1-W) = \left[1 - \frac{2.42\, C_{d_o}^{1/2}}{\xi + 0.3} \cos^2\left(\frac{\pi}{2}\,\frac{\zeta'}{\zeta}\right)\right]^{1/2} \qquad [9]$$

It is seen in Equation [7] that maximum loss of dynamic pressure varies inversely as the first power of distance ξ downstream. For our purpose, the most important limitation of estimating the wake factor from Equation [9] is the fact that the relation was derived from experiments with finite wings. However, aspect ratios for the test wings[8] range from about 3 to 10.

If the wake centerline is assumed to coincide with the centerline of the trailing vortex sheet, the wake centerline at any given longitudinal position can be located by the empirical equation[10]

$$\frac{d}{c} = C_L \left[\left(\frac{m}{c} - 0.2\right) f + 0.025\right] \qquad [10]$$

$\frac{m}{c}$	f
0.30	0.09
0.20	—
0.15	0.34
0.10	0.28

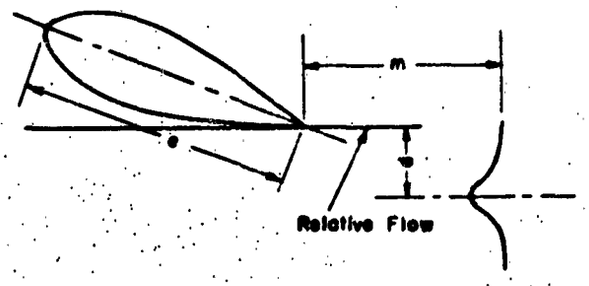

Figure 2 – Position of Wake Centerline Relative to Hydrofoil

The arrangement and quantities are shown schematically in Figure 2. The empirical constant *f* which is tabulated in Figure 2 was derived in Reference 10 from studies of numerous wakes.

PROPELLER-THRUST FLUCTUATIONS

It is assumed that propeller-thrust fluctuations due to a nonuniform wake distribution over the propeller disk can be estimated by calculating quasi-steady propeller forces. An adaptation of Burrill's strip-theory method of calculation for marine propellers is used here to calculate these quasi-steady state forces.[11,12] In this method, unsteady effects are not considered; i.e., when the frequency of oscillating velocities is small, a rotating propeller in a variable wake is assumed to experience lift and drag at each blade element as if the blade were in steady flow at each instant. The various angles and velocities at a typical propeller-blade section are given in Figure 3. When placed in the wake of a hydrofoil with lift, a propeller will have a downwash component added to the section inflow velocity. In general, variations per revolution in propeller total thrust are essentially zero due to uniform

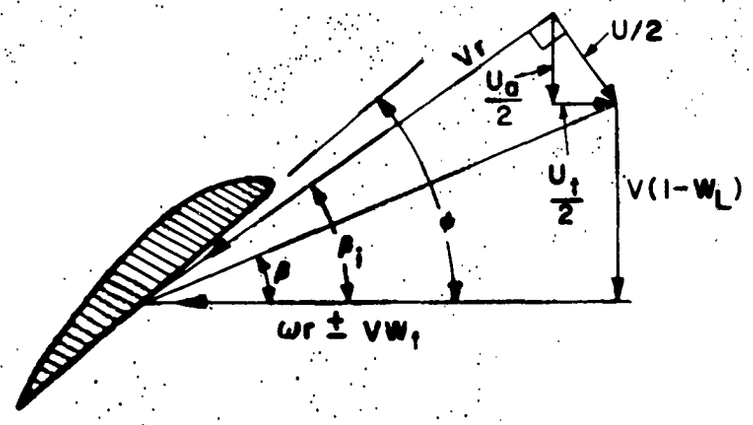

Figure 3 – Velocity Diagram of a Propeller-Blade Section

downwash because only nonlinear effects acting on the section characteristics contribute to the thrust variation per revolution. For the most part, section characteristics may be obtained from Reference 11.

COMPUTED EXAMPLE

WAKE

A nominal value of the drag coefficient (C_{d_o} = 0.01)* was used to compute a wake distribution at several positions behind a NACA 16-309 foil.[13] The augmented resistance of the subject foil was obtained for C_L values of 0 and 0.3 (design lift). In this range of lift coefficient (α_{L_o} = −2.04 deg to α = 0.92 deg), the effect of section-drag coefficient on the wake distribution is not too important because of the small changes in C_{d_o} that occur in this region.[13] Likewise, the downward displacement of the wake centerline at design lift is calculated from Equation [10] to be negligible at ξ = 0.15 and 0.30. Wake profiles as computed from Equations [6] and [9] are depicted in Figure 4 for several positions downstream from the 16-309 hydrofoil. These results are used in the calculation of propeller-fluctuating thrust.

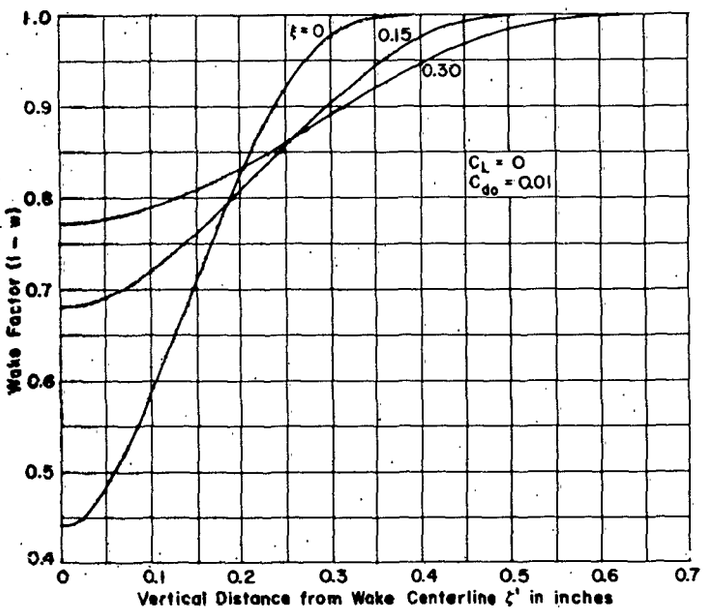

Figure 4 – Wake Profiles at Several Positions behind a NACA 16-309 Hydrofoil

*The nominal value 0.01 is confirmed by the resistance-test results in Figure 12. In Figure 12, the wetted surface is twice the plan-form area and, therefore, $C_{d_o} = 2C_f$.

Disturbing potential velocities $W_P V$ from the 16-309 hydrofoil were obtained from a high-speed computer program of the Douglas Aircraft Company, El Segundo, California, and is known at the Taylor Model Basin as the Douglas program. In the method of calculating potential flows with circulation as developed by Douglas, a solution is secured by specifying a combination of a rectilinear flow, a crossflow, and a vortex flow. The two-dimensional potential flow behind the 16-309 hydrofoil is presented graphically in Appendix A for $C_L = 0$ and $C_L = 0.3$ at several distances (ξ) downstream. The ordinates of the curves in these figures are the potential wake fraction W_P at the propeller. Following D.W. Taylor, a general wake fraction is defined as $W = \dfrac{V - V_a}{V}$.

PROPELLER-FLUCTUATING THRUST

Computational results for fluctuating total thrust are presented graphically in Figure 5 for the following propeller positions behind the NACA 16-309 hydrofoil: Foil on propeller-

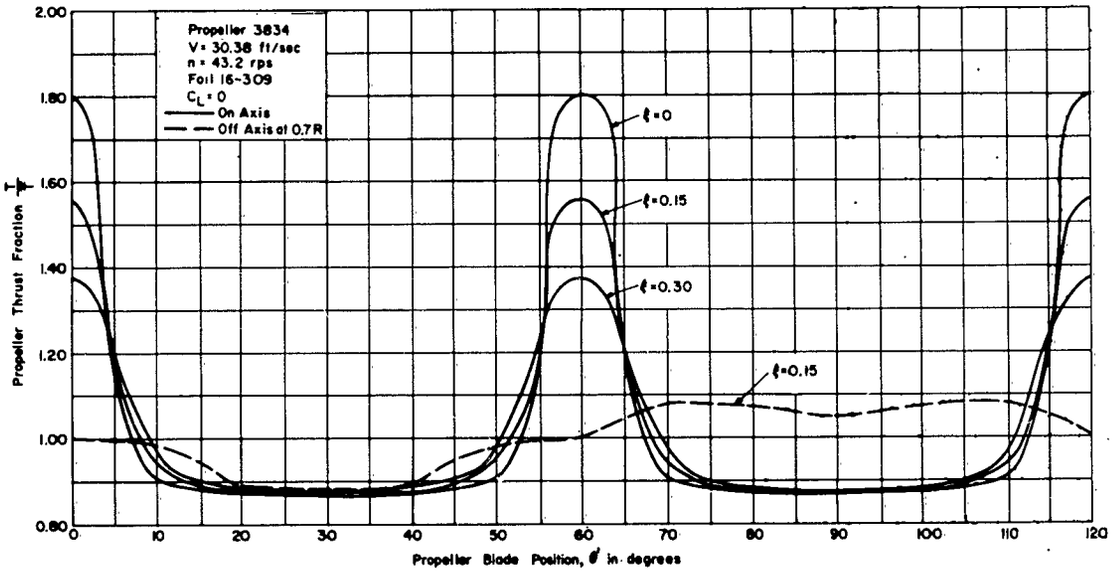

Figure 5 – Curves of Fluctuating Total Thrust for Propeller 3834

shaft axis with $\xi = 0$, 0.15, and 0.30; and foil off the propeller-shaft axis at $x = 0.7$ for $\xi = 0.15$. It is noted that, when the shaft axis of a 3-bladed propeller is parallel to the direction of motion and coincides with a symmetrical wake centerline, the period is 60 deg because of symmetry. If a 3-bladed propeller is off center, the period is $\dfrac{360}{3} = 120$ deg. These total thrust curves are used subsequently to calculate interaction forces.

A harmonic analysis of the fluctuating thrust curves was made using a 12-ordinate scheme given by Scarborough.[14] The dimensional Euler coefficients a_n and b_n are given in Table 1 for each propeller-hydrofoil arrangement. It is noted that only cosine terms appear in

TABLE 1

Harmonic Coefficients in the Series Expansion

Harmonic Coefficients	Foil on Propeller Axis*			Foil off Axis at $x = 0.7$**
	$\xi = 0.00$	$\xi = 0.15$	$\xi = 0.30$	$\xi = 0.15$
a_0	46.2	46.6	47.3	53.37
a_1	10.66	10.28	9.57	0
a_2	8.66	6.73	5.58	1.620
a_3	6.52	4.03	2.58	0
a_4	4.98	2.50	0.683	- 0.487
a_5	4.17	1.68	- 0.303	0
a_6	1.97	0.666	- 0.308	- 0.589
b_1	0	0	0	- 5.17
b_2	0	0	0	0
b_3	0	0	0	- 0.175
b_4	0	0	0	0
b_5	0	0	0	0.507

*Period = 60 degrees

**Period = 120 degrees

the expansion for the foil on the propeller shaft axis for $\xi \leq 0.3$. This is caused by the symmetry of the cosine-squared wake distribution and its location. For the off-axis position, sine and cosine terms alternate. The Euler coefficients can be combined as

$$A_n \sin (nz + \phi_n)$$

where

$$A_n = \sqrt{a_n^2 + b_n^2}$$

and

$$\phi_n = \tan^{-1}\left(\frac{a}{b}\right)_n$$

Plotted in Figure 6 as a function of ξ are the resultant positive harmonic coefficients A_n expressed as a fraction of the direct component for each on-axis condition. When the propeller has reached the $\xi = 0.30$ position downstream, apparently only the first, second, and third resultant harmonics contribute significantly to total thrust fluctuation. The coefficients A_n for the foil off the

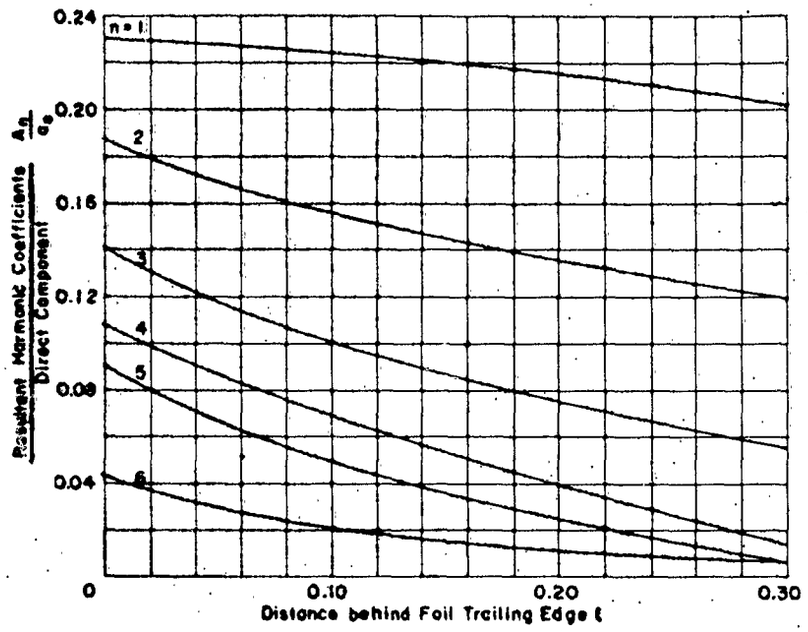

Figure 6 – Variation of Resultant Harmonic Coefficients of Fluctuating Thrust with ξ

Curves are for foil on propeller-shaft axis.

propeller axis ($x = 0.7$) are:

$\xi = 0.15$	
Order	$\frac{A_n}{a_0}$
1	0.0970
2	0.0304
3	0.0033
4	0.0091
5	0.0095
6	0.0110

THRUST DEDUCTION

Equations [3] and [5] are evaluated numerically using Simpson's rule. The functions η^*/V_a and η_1^*/V_a are calculated using the appropriate total-thrust curve in Figure 5. In calculating η_1^*/V_a, the direct component may be obtained directly from Table 1. Appropriate values of W_P are read from the curves in Appendix A and, with the input data as outlined, numerical solutions were obtained for several assumed values of effective wake factor $(1 - W)$. Resulting values of C_D, C_{D_1}, and $C_{D_2} = C_D - C_{D_1}$ are tabulated in Table 2 for several propeller-hydrofoil arrangements and conditions.

TABLE 2

Computed Augmented-Drag Coefficients for Various Propeller-Hydrofoil Arrangements and Conditions

ξ	Foil Lift	$C_L = 0.0$			$C_L = 0.3$		
	$(1-W)$	$10^2\, C_D$	$10^2\, C_{D_1}$	$10^2\, C_{D_2}$	$10^2\, C_D$	$10^2\, C_{D_1}$	$10^2\, C_{D_2}$
0	0.80	1.734	1.645	0.089	1.731	1.554	0.177
	0.90	1.383	1.284	0.099	1.386	1.241	0.145
	0.97	–	–	–	1.191	1.074	0.117
0.15	0.80	1.026	1.044	$\simeq 0$	1.043	1.060	$\simeq 0$
	0.90	0.8204	0.8340	$\simeq 0$	0.8334	0.8472	
	0.97	–	–	–	0.7151	0.7334	
0.30	0.80	0.6808	0.6833	$\simeq 0$	0.6701	0.6658	
	0.90	0.5433	0.5458	$\simeq 0$	0.5353	0.5373	
	0.97	–	–	–	0.4581	0.4652	$\simeq 0$
Foil off Axis at $x = 0.7$							
0.15	0.80				1.340	1.348	$\simeq 0$
	0.90				1.071	1.078	$\simeq 0$
	0.97				0.9204	0.9253	$\simeq 0$

In Figures 7 and 8, the thrust-deduction curves were computed using the augmentation coefficients of Table 2 and the relations

$$t = \frac{2C_D}{\overline{C}_T \pi (1-W)} \quad , \quad t_1 = \frac{2C_{D1}}{\overline{C}_T \pi (1-W)}$$

The effects of propeller-hydrofoil spacing, wake, fluctuating thrust, and foil lift are all apparent in these figures. For $(1 - W) = 0.90$, which is more likely to be obtained in practice, the effect on t and t_1 of going from $C_L = 0$ to $C_L = 0.3$ is not important because the effect on total system $(1 - t)$ is quite small even in the vicinity of $\xi = 0$.

Considering conditions at design-lift coefficient ($C_L = 0.3$), the influence of spacing ξ on the thrust-deduction coefficients t and t_1 is significant. In going from $\xi = 0$ to $\xi = 0.3$, t and t_1 are reduced from an order of magnitude of approximately 0.05 to approximately 0.02. The higher the effective wake W, the more pronounced is this reduction. The contribution of the fluctuating part of the total propeller thrust on t is apparent only at or near the foil trailing edge ($\xi = 0$). Relative to the on-axis condition, the off-axis curve in Figure 8 appears parallel and displaced upwards about 0.005 units. To further investigate off-axis performance, additional calculations were made at $x = 0.4$ (in lift direction) based on an average thrust-loading coefficient $\overline{C}_T = 0.1979$. The average thrust coefficient is based on the direct thrust components given in Table 1, and an assumed value of 0.90 for the wake factor (validated later by

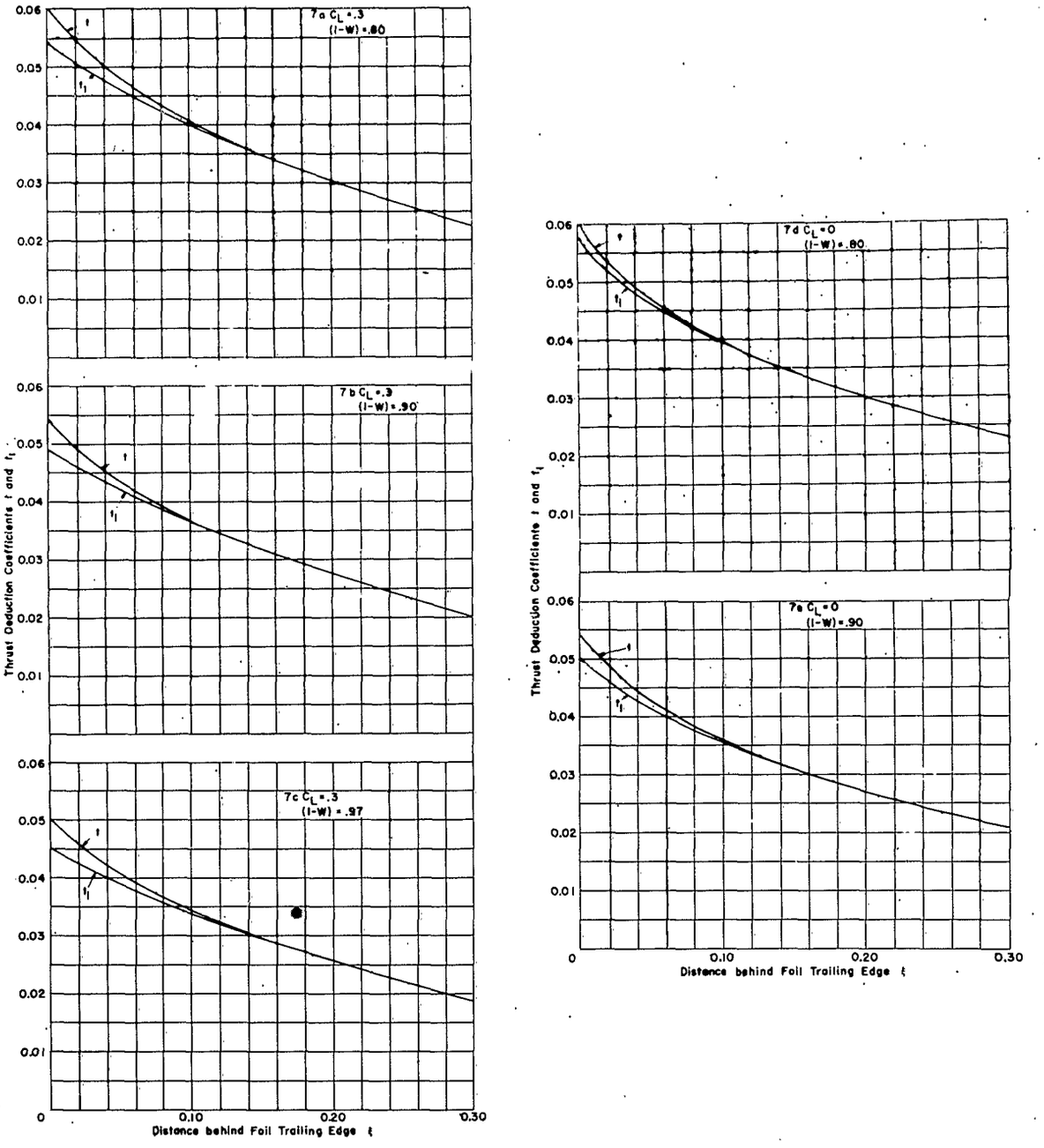

Figure 7 – Computed Thrust-Deduction Coefficient versus ξ for Hydrofoil 16-309 and Propeller 3834

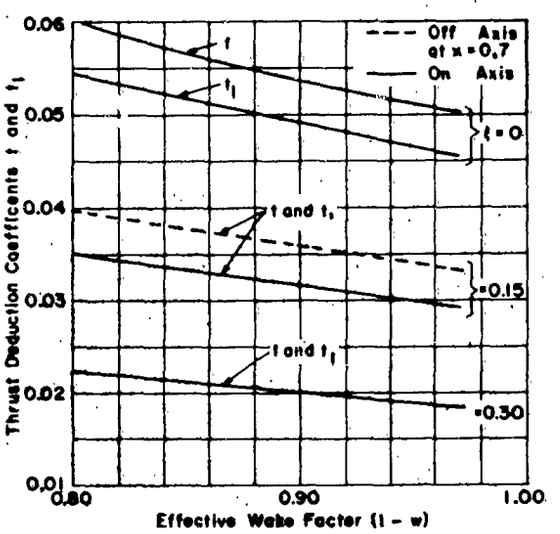

Figure 8 – Computed Thrust-Deduction Coefficient versus $(1-W)$ at $C_L = 0.3$ for Hydrofoil 16-309 and Propeller 3834

the experimental results in Table 4). A computed value of $t = 0.036$ was obtained for $x = 0.4$. This result is the same as that obtained for the off-axis condition at $x = 0.7$ (see Figure 8). The effective wake is essentially constant within the range of $x = 0.4$ to 0.7; consequently, the average thrust is the same at the same revolutions. This means that the same sink strength combines with a weaker disturbing field W_P to give a lower thrust deduction. The accuracy to which this weaker potential field can be determined is questionable. In any event, a theoretically obtained curve of thrust deduction with off-axis position would tend to zero for foil locations out of the propeller disk.

EXPERIMENTS

DESCRIPTION OF PROPELLER AND HYDROFOIL

The TMB stock propeller selected for the propeller-hydrofoil configuration was 3834, a three-bladed aluminum propeller with a diameter of 8 in. A drawing of this propeller is shown in Figure 9. The NACA 16-309 high-lift and low-drag section was used for the hydrofoil (TMB Model H-41) which corresponds to the submerged hydrofoils of Navy's first operational hydrofoil patrol boat PC(H). The offsets for the NACA 16-309 section are tabulated in Table 3. The ratios foil chord to propeller diameter c/d and foil maximum thickness to propeller diameter t/d are 1.67 and 0.15, respectively.

Model H-41 was equipped with a removable nacelle of 3.5-in. diameter (TMB Series-58 shape) and an adjustable tail flap. Provision was made for removing segments of the foil from

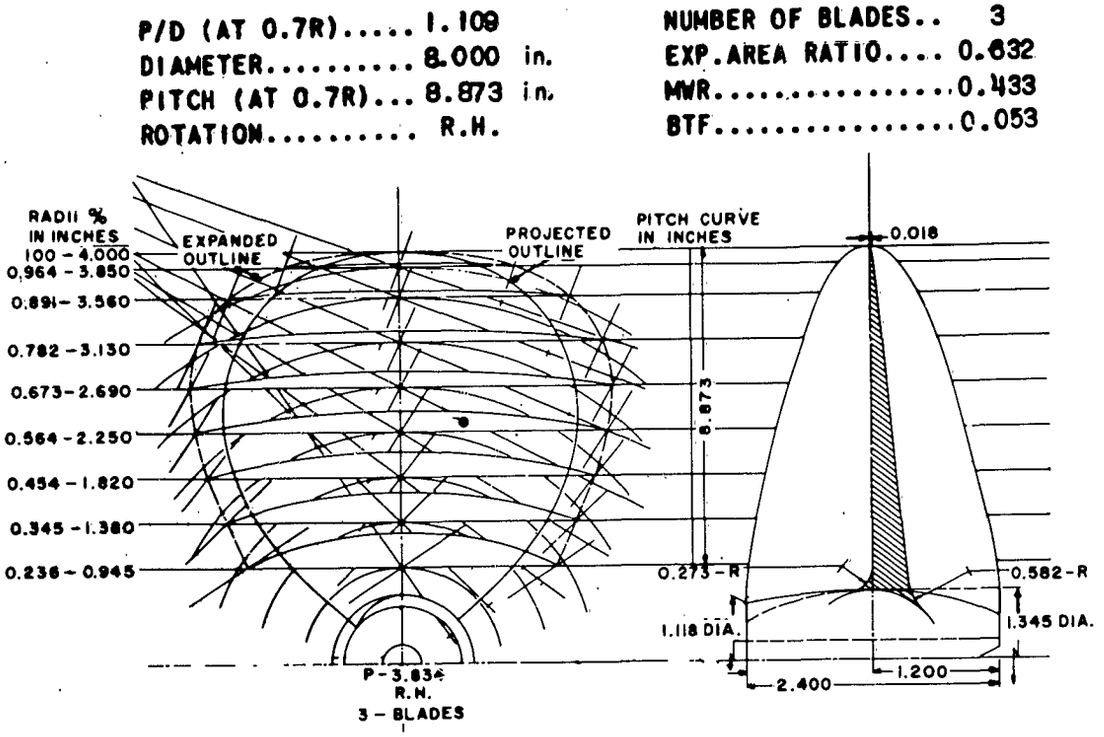

Figure 9 – Drawing of TMB Propeller 3834

TABLE 3

Offsets for NACA 16-309 Section, TMB Model H-41

Distance from Nose Chords	Distance from Nose Inches	Upper Surface Y Inches	Lower Surface Y Inches
0.000	0.0000	0.0000	0.0000
0.050	0.6666	0.3145	0.1876
0.100	1.3333	0.4492	0.2423
0.200	2.6666	0.6256	0.3072
0.300	3.9999	0.7364	0.3476
0.400	5.3332	0.8000	0.3709
0.500	6.6665	0.8206	0.3793
0.600	7.9998	0.7980	0.3689
0.700	9.3331	0.7216	0.3322
0.800	10.666	0.5790	0.2607
0.900	11.999	0.3552	0.1483
0.950	12.666	0.2048	0.0781
1.000	13.333	0.0000	0.0000

the lower end. With these features incorporated in the hydrofoil, the augmented resistance could be determined for test conditions which represent, with and without nacelle, infinite span and semi-infinite span. A parameter designated the span ratio l/L was used to define the geometry of the semi-infinite span conditions. In the span ratio, l is the foil span measured from the axis of the water tunnel jet to the free end of the foil and L is the foil span measured from the top of the water tunnel jet to the free end of the foil.

ARRANGEMENT AND INSTRUMENTATION FOR TESTS

Figure 10 shows hydrofoil Model H-41 and the drag dynamometer as assembled prior to conducting tests in the 24-in. water tunnel. Figure 11 shows the arrangement for a typical test of the hydrofoil and propeller in this tunnel. The foil was mounted vertically across the tunnel jet. A column which was secured to a drag dynamometer was connected (outside the tunnel jet) to the upper end of the foil. The lower end of the foil extended beyond the jet boundary and was free. The hydrofoil and propeller were not mechanically connected so the foil-resistance augment is obtained directly from the resistance measurements.

The drag dynamometer was of the TMB magnigage type and had a linear calibration within the range of drag and lift forces encountered in the investigation. The accuracy of the drag measurements was $\pm\frac{3}{4}$ to ± 1 percent of full load. Accuracy of propeller measurements, using the 10-hp dynamometer for the 24-in. water tunnel was also about ± 1 percent of full load.

TEST PROCEDURE

Resistance tests with and without the propeller were conducted at atmospheric pressure for each hydrofoil configuration and position. All tests were conducted at a constant speed of 14 knots except Test 4 (flap-angle variation) which was run at a speed of 12 knots because excessive vibration was encountered at 14 knots. The constant-speed tests with the propeller were conducted by measuring propeller thrust and torque and foil resistance over a range of propeller rpm which corresponded to J values of about 0.7 to 1.1. In addition to constant-speed runs, the effect of test Reynolds number (speeds of 6 to 14 knots) on the hydrofoil resistance for Test 1 was investigated for the purpose of establishing the adequacy of test Reynolds number.

DISCUSSION OF RESULTS

Thrust-deduction coefficients versus propeller-speed coefficient are given in Appendix B for each test. Experimental data points are plotted for each curve. Although the results are discussed primarily in terms of faired thrust-deduction coefficients for a propeller-speed coefficient $J = 0.9$ (corresponds closely to maximum propeller efficiency), a wide range of J's was covered in order to provide additional data for fairing purposes and to investigate the effect of J on t more completely.

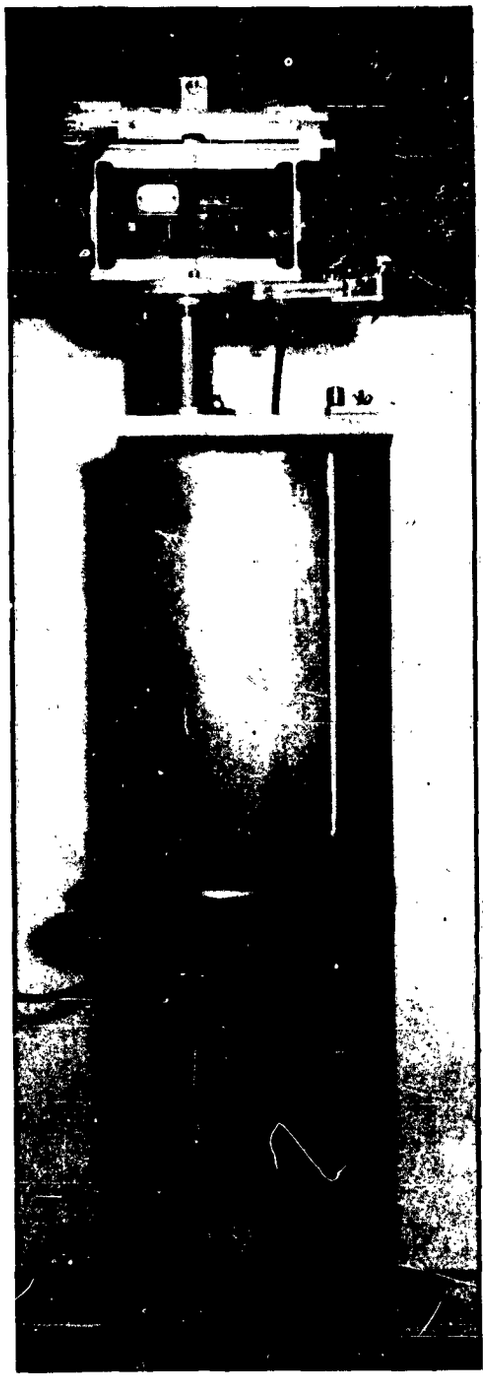

Figure 10 – TMB Hydrofoil Model H-41 and Dynamometer Assembly

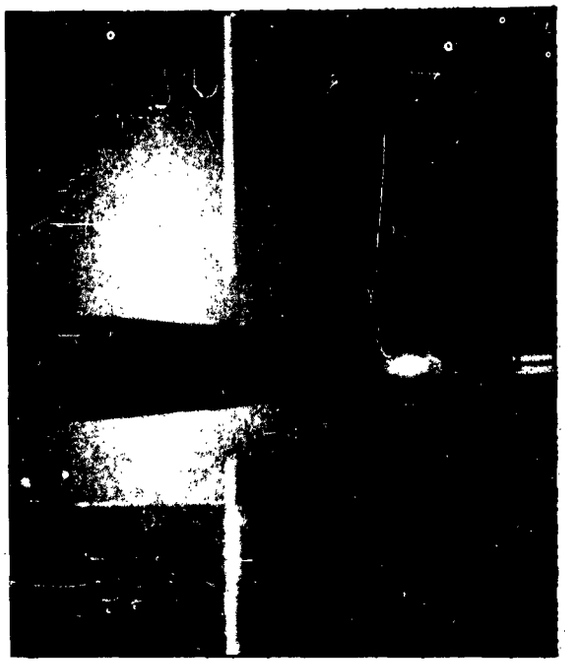

Figure 11a – Test 3 with Foil at $\xi = 0.30$ Position

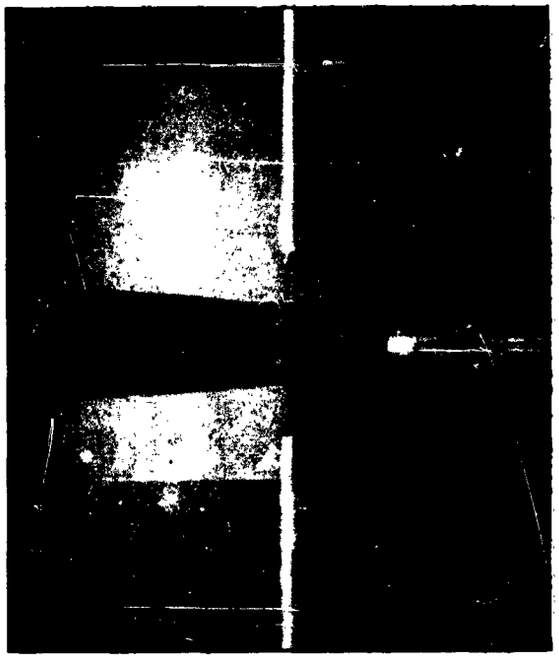

Figure 11b – Test 3 with Foil at $\xi = 0.15$ Position

Figure 11 – Model H-41 Installed for Testing in 24-Inch Water Tunnel

The results of tests to determine Reynolds effect are presented in Figure 12 as curves of total-resistance coefficient C_t versus Reynolds number R_n with

$$C_t = \frac{R_t}{\frac{1}{2}\rho S V^2}$$

and

$$R_n = \frac{Vc}{\nu}$$

It is seen that, for $\xi = 0.15$ and $\xi = 0.30$, the C_t curves appear to parallel the Schoenherr turbulent frictional-resistance line for a flat plate.

Table 4 summarizes the test conditions and corresponding experimental values of thrust-deduction coefficient t and wake factor $(1-W)$. A comparison of the experimental values of $(1-W)$ for Test 2 and the computed on-axis data which are cross-plotted in Figure 8 shows that the t values agreed for both the $\xi = 0.15$ and $\xi = 0.30$ positions:

		Thrust-Deduction Coefficient	
ξ	$(1-W)$	Theoretical	Experimental
0.15	0.910	0.031	0.031
0.30	0.919	0.019	0.018

Examination of the off-axis experimental results and the theoretical results that are plotted in Figure 13 indicates that the experimental curve showed a slight decrease in t (from 0.031 to 0.021 in going from $x = 0$ to $x = 0.7$ in the lift direction). This reduction in t is to be expected and, of course, t becomes zero when the foil is moved completely away from the propeller field. Although the theoretically obtained thrust deduction remained essentially constant at $t = 0.036$ for a range of x comparable to the experiments, the order of magnitude for t was correct.

The most important result shown by the remaining test data in Table 4 and in Figures 14 and 15 is the small change in one-minus-the-thrust deduction (a negligible effect on the total system due to thrust-deduction variations) for the various configurations. This result confirms, of course, the analytical procedure. Figure 15 shows a negligible change in t from $l/L = 0.3$ to $l/L = 0.5$ which approximates an infinite aspect ratio. Since the span ratio was varied by removing segments of the span from the free end only, the increase in foil drag due to the flow at one tip was about one-half of that which would occur for a usual finite wing.

The following additional remarks are made relative to the experimental data:

1. The experimental results confirmed the theoretical result which indicated that the effect of foil lift (C_L maximum = 0.3) on thrust deduction can be disregarded except at or near zero clearances.

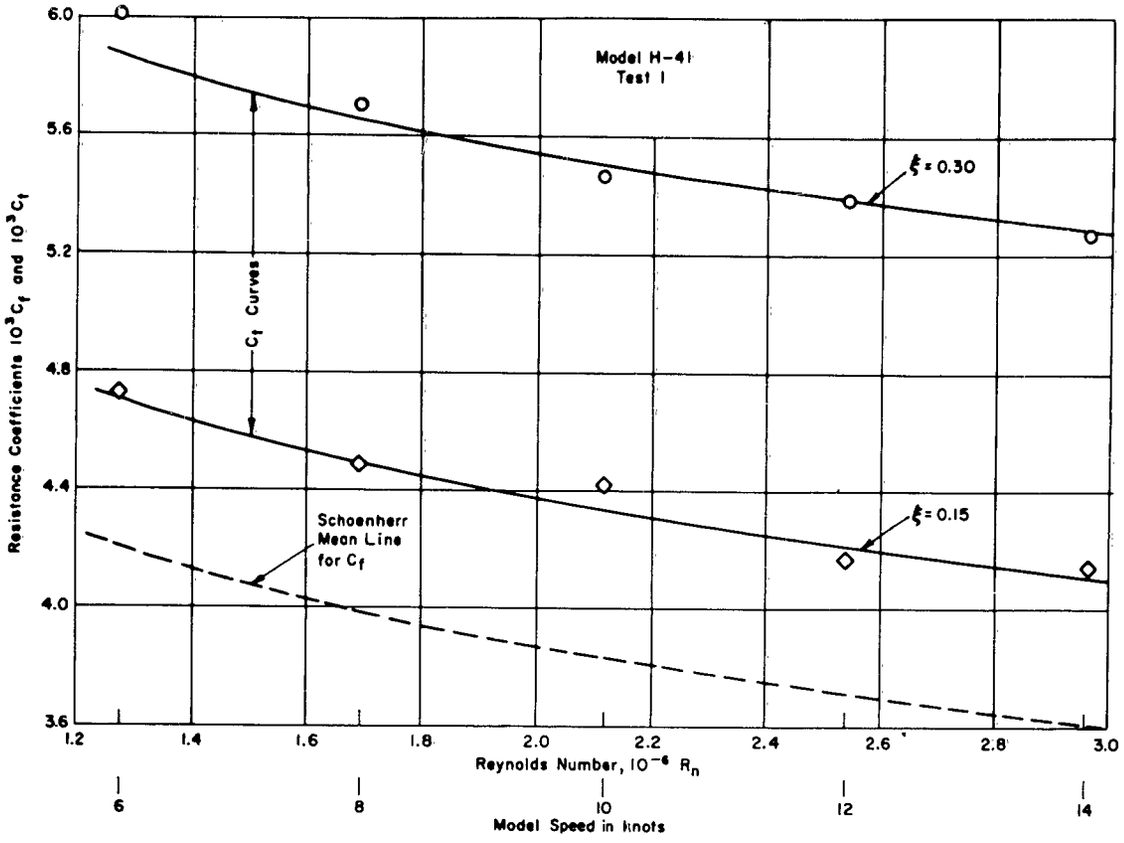

Figure 12 – Total-Resistance Coefficient versus Reynolds Number for Model H-41, Test 1

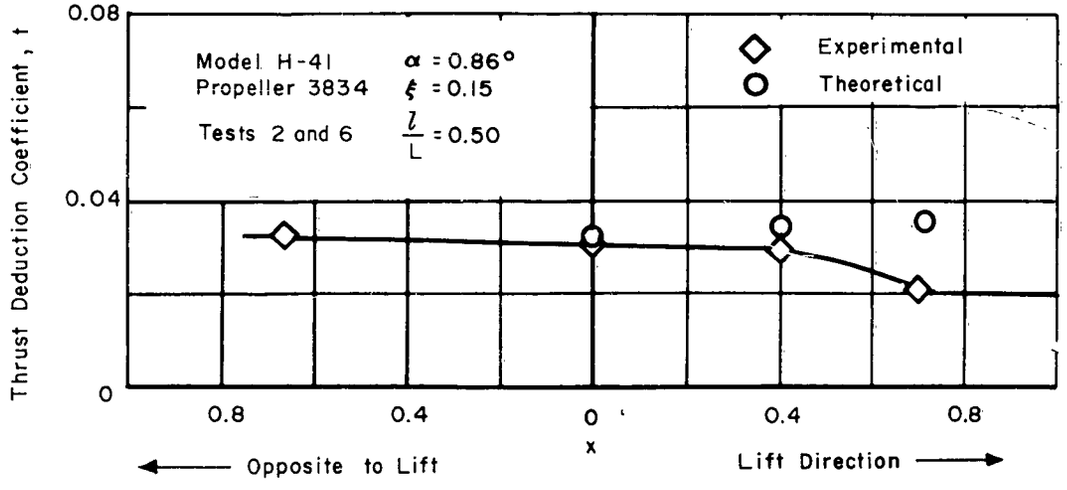

Figure 13 – Variation of Thrust-Deduction Coefficient with Off-Axis Position, Tests 2 and 6

TABLE 4

Summary of Test Conditions and Results

Test Number	Conditions							Thrust Deduction t	1-Wake Fraction $(1-W)$	Remarks*
	Angle of Attack α Deg	Estimated Lift Coefficient C_L	Position ξ	Span Ratio l/L	Flap Angle Deg	With Nacelle	Without Nacelle			
1	−2.05	0	0.15	0.50	0		X	0.031	0.908	On Axis
1	−2.05	0	0.30				X	0.018	0.919	On Axis
2	0.86	0.3	0.15				X	0.031	0.910	On Axis
2	0.86	0.3	0.30				X	0.018	0.919	On Axis
3	−0.20	0.2	0.15			X		0.043	0.890	On Axis
3	−0.20	0.2	0.30			X		0.024	0.910	On Axis
3	0.86	0.3	0.30		0	X		0.024	0.910	On Axis
4	0.50	0.56	0.15		5	X		0.044	0.885	On Axis
4	0.50	0.73		0.50	10	X		0.05	0.885	On Axis
5	−0.20			0.281	0	X		0.04	0.905	On Axis
5	−0.20			0.420		X		0.046	0.890	On Axis
6	0.86	0.3		0.50			X	0.03	0.900	Off Axis (0.4R in lift direction)
6	0.86	0.3		0.50			X	0.021	0.900	Off Axis (0.7R in lift direction)
6	0.86	0.3	0.15	0.50	0		X	0.032	0.913	Off Axis (0.66R opposite to lift direction)

*The faired values of t and $(1-W)$ are for $J = 0.90$.

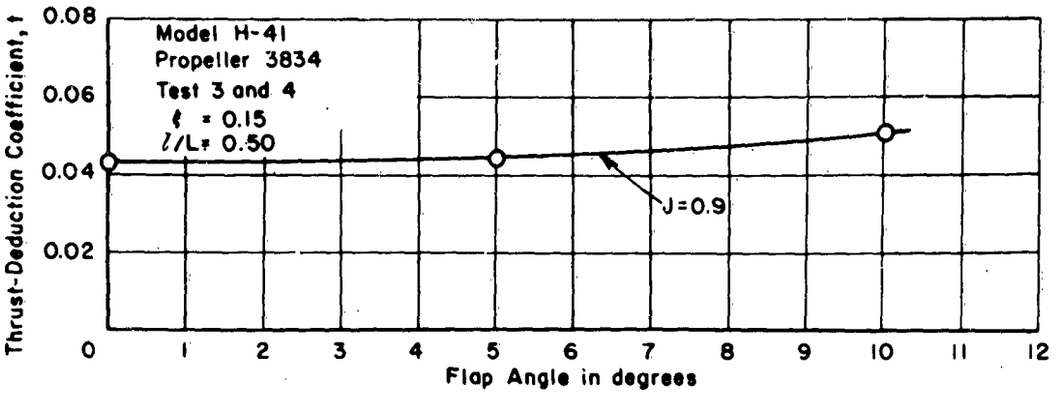

Figure 14 – Thrust-Deduction Coefficient versus Flap Angle for Foil with Nacelle, Tests 3 and 4

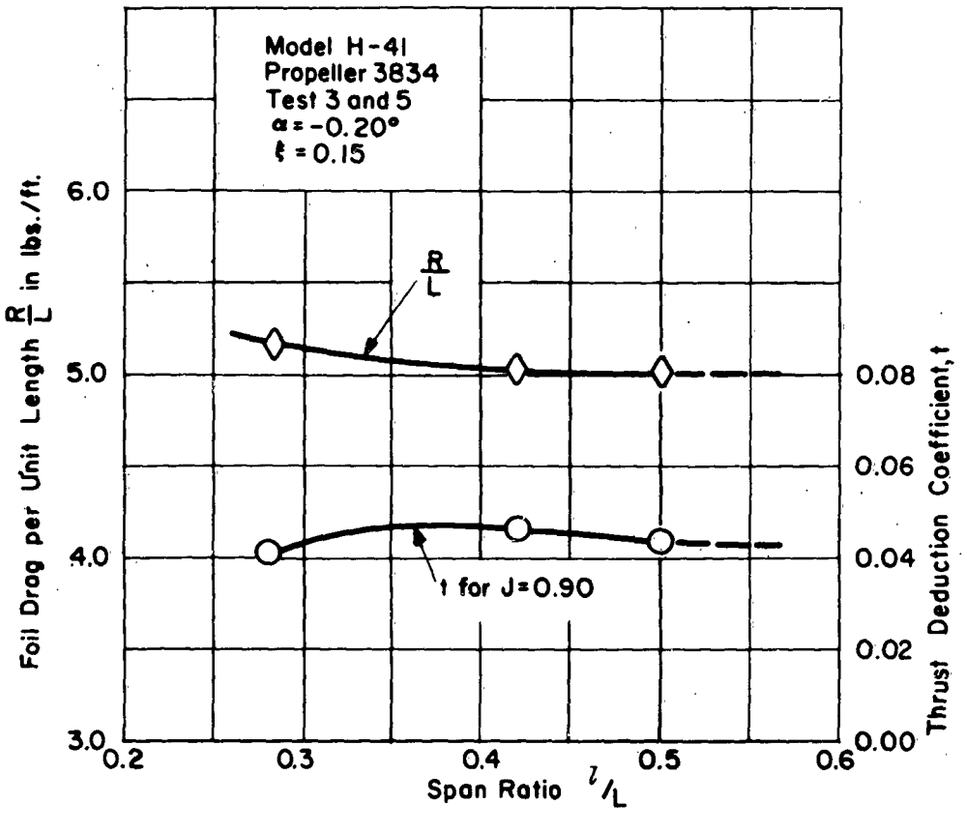

Figure 15 – Variation of Thrust-Deduction Coefficient and Foil Drag per Unit Length with Span Ratio for Foil with Nacelle, Tests 3 and 5

2. Within the normal operating range of the propeller, the effect of propeller-speed coefficient on the thrust-deduction coefficient was nil.

CONCLUDING REMARKS

A method which is based on Lagally's steady-motion theorem was derived and used to calculate the resistance augmentation for a submerged hydrofoil. In the method, mathematical singularities are derived from propeller-fluctuating thrusts as estimated from quasi-steady theory using empirically obtained wake data. The disturbing foil velocities for potential flow are obtained from a high-speed computer program. A harmonic analysis of the total fluctuating thrust curves computed for a three-bladed propeller indicated that, when the propeller was positioned about 0.3 times the foil chord downstream from the trailing edge and on an axis through the foil trailing edge, only the first, second, and third resultant harmonics contributed significantly to total thrust fluctuation. Computed and experimental thrust-deduction results for several hypothetical on-axis and off-axis arrangements and conditions were in good agreement.

The most salient features concerning the effects on thrust deduction of the parameters and conditions investigated are summarized as follows:

1. The contribution of the fluctuating part of the propeller total thrust to the thrust deduction was important when the propeller was located at or near the foil trailing edge.

2. Clearance between the foil trailing edge and the propeller was important. In going from zero clearance to 0.3-chord length, one-minus-the-thrust deduction varied from 0.946 to 0.980.

3. In the range of lift coefficients from zero to design lift (C_L = 0.3), the influence of lift on one-minus-the-thrust deduction was generally negligible.

4. Within the normal operating range of the propeller, the effect of propeller-speed coefficient on thrust deduction was nil.

5. Within the range of investigation, there was little effect on the total system due to thrust-deduction variations with foil-span ratio (0.28 to 0.50) and foil flap angle (0 to 10 deg).

APPENDIX A

GRAPHS OF COMPUTED POTENTIAL WAKE FRACTION

Figure 16 – Computed Potential Wake Fraction, Foil 16-309, $C_L = 0$, $\alpha = -2.05$ Degrees

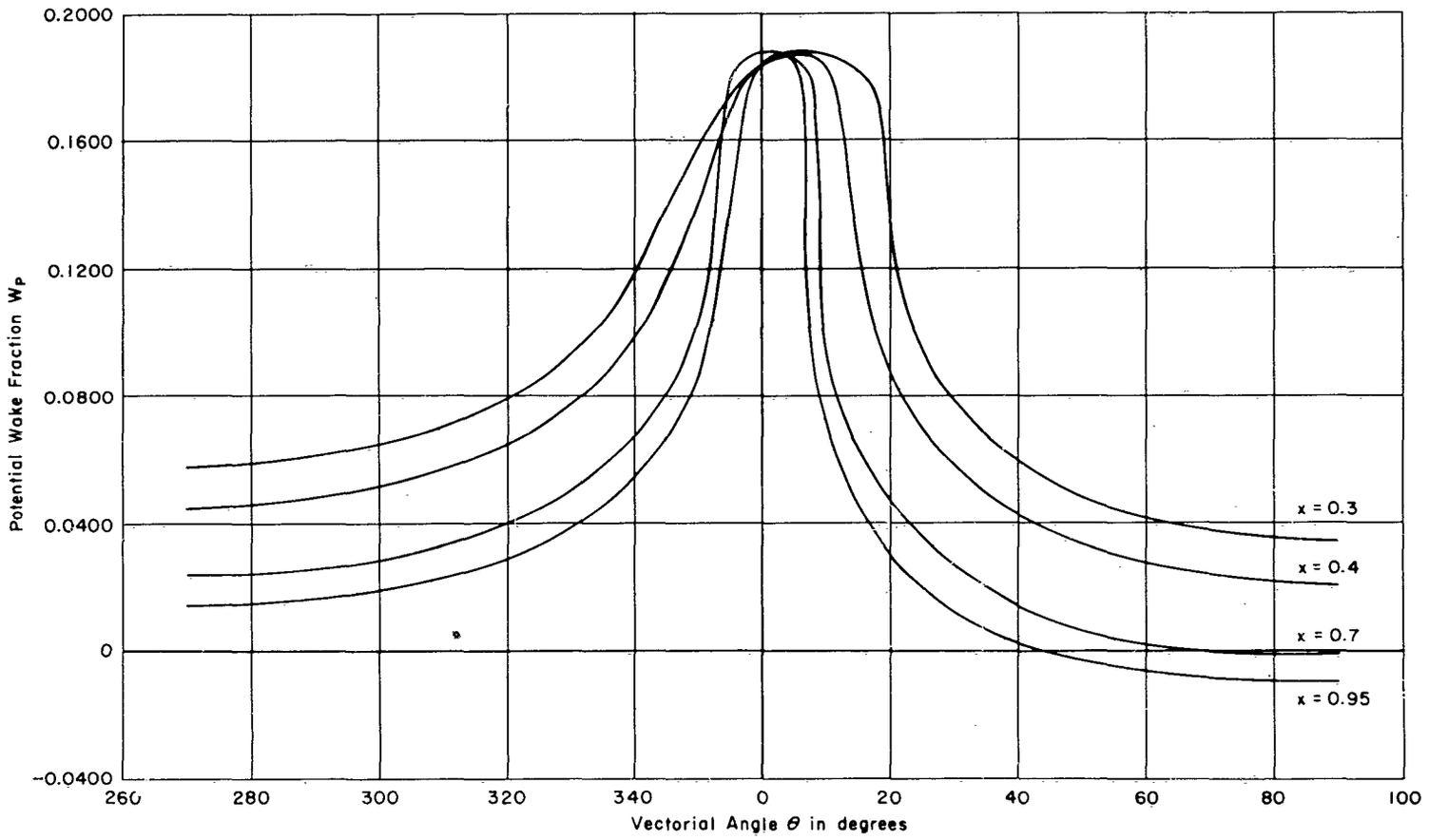

Figure 16a – $\xi = 0$

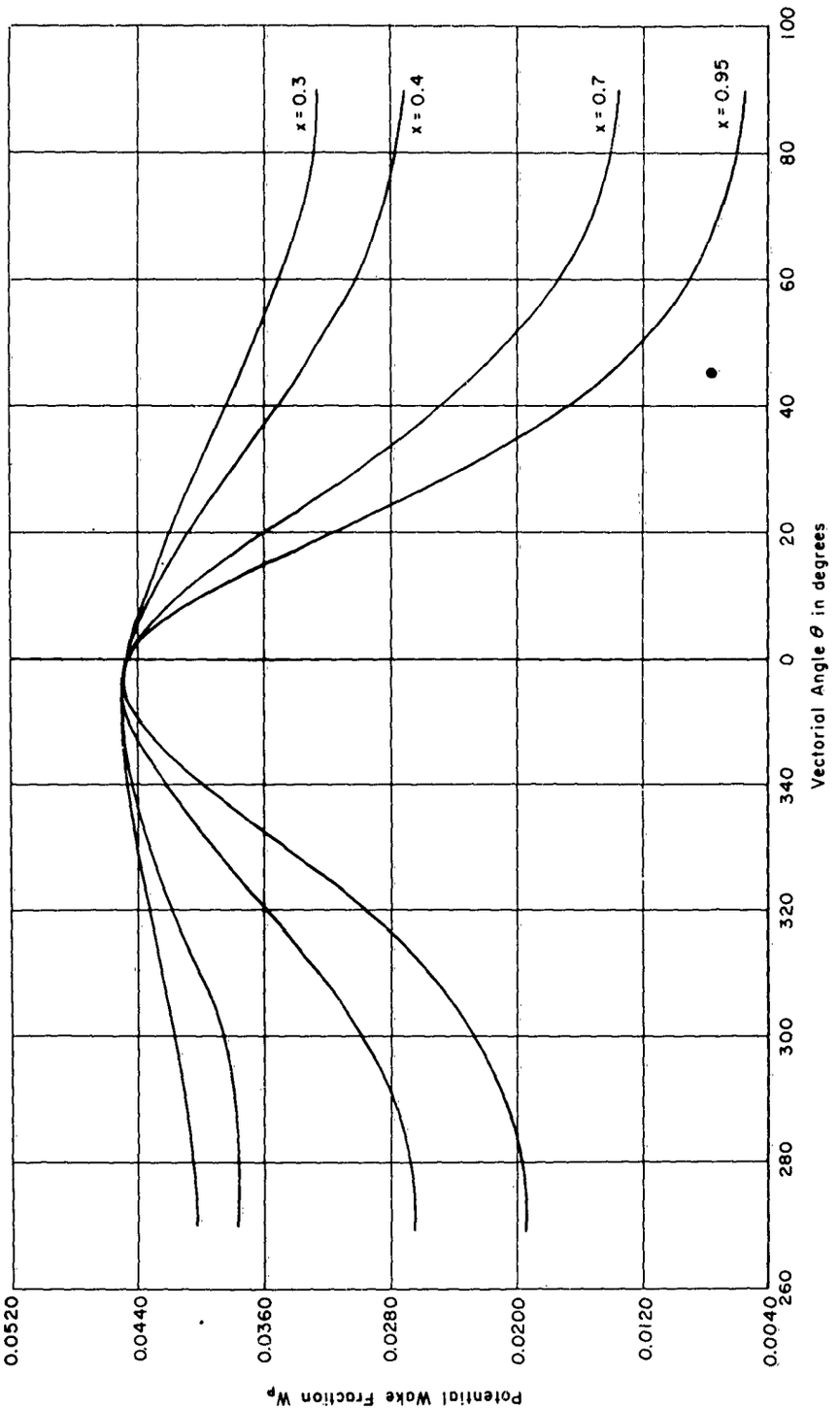

Figure 16b – $\xi = 0.15$

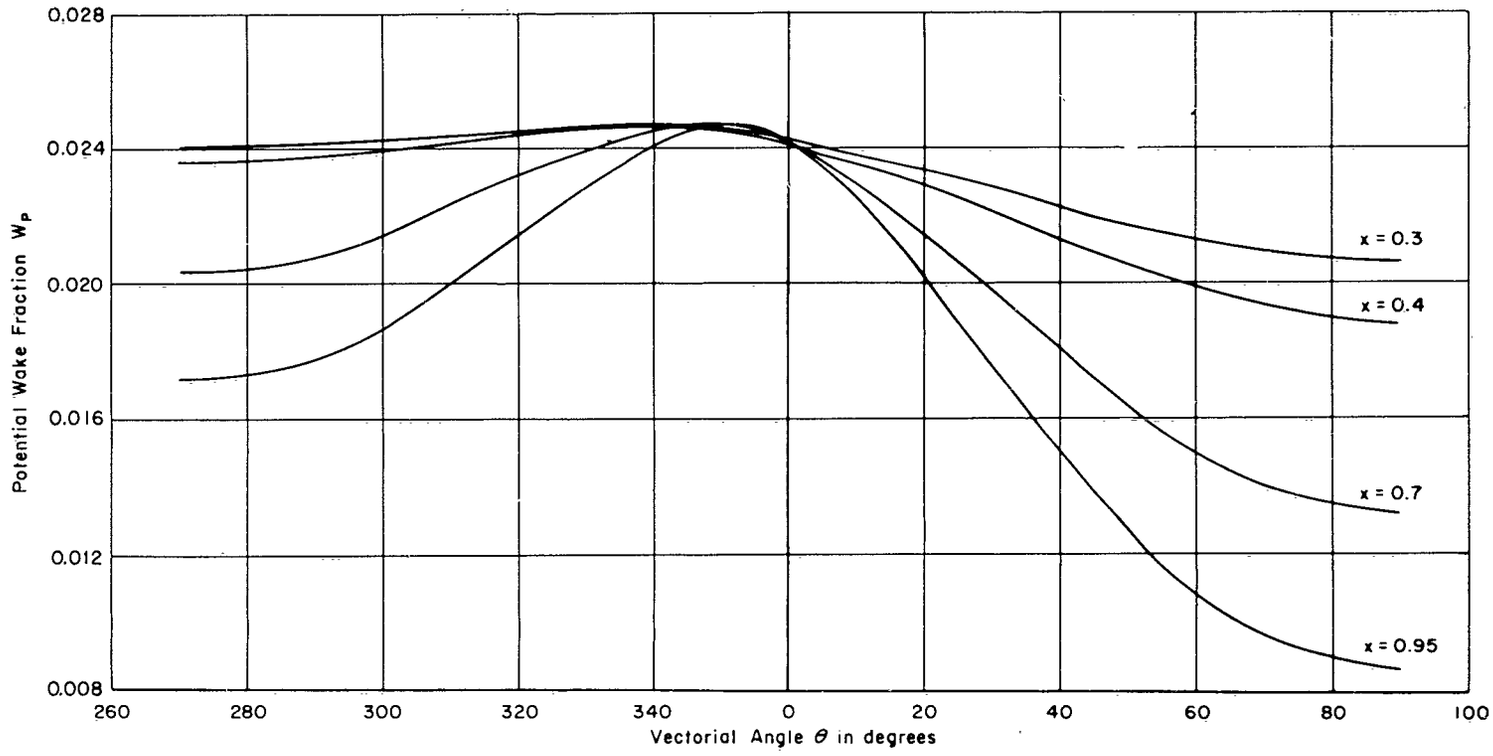

Figure 16c – $\xi = 0.3$

Figure 17 – Computed Potential Wake Fraction, Foil 16-309, $C_L = 0.3$, $\alpha = 0.92$ Degrees

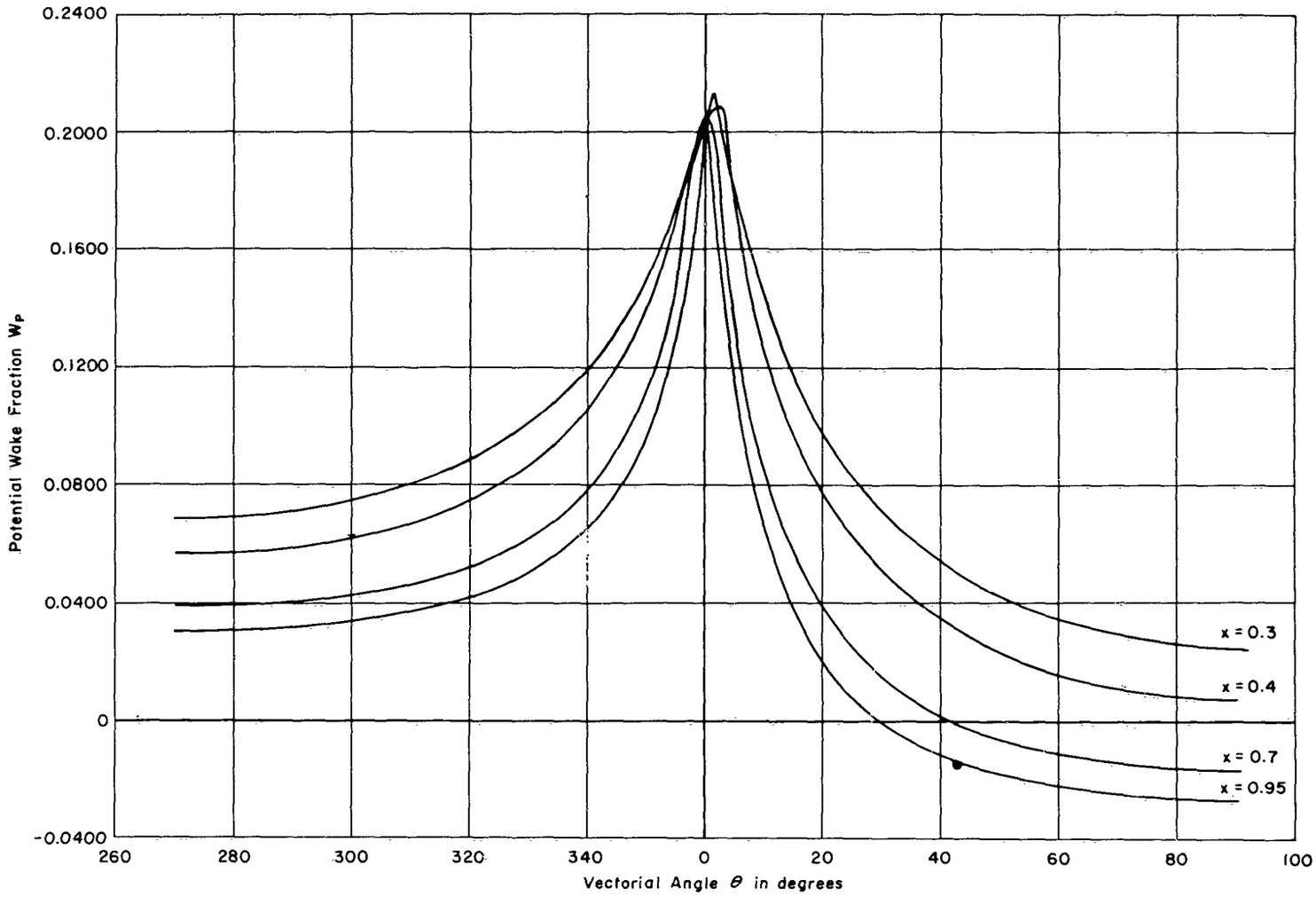

Figure 17a – $\xi = 0$

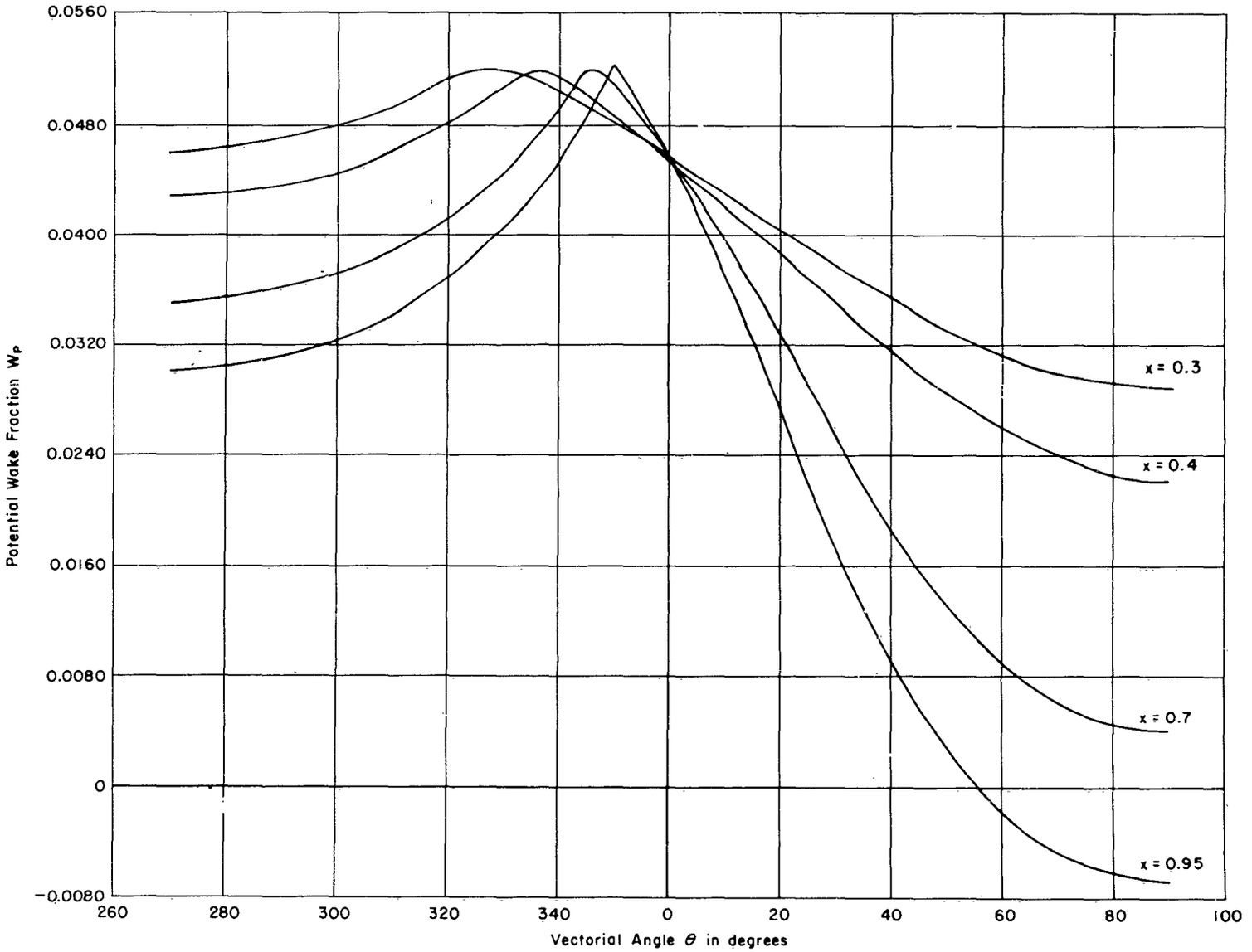

Figure 17b – $\xi = 0.15$

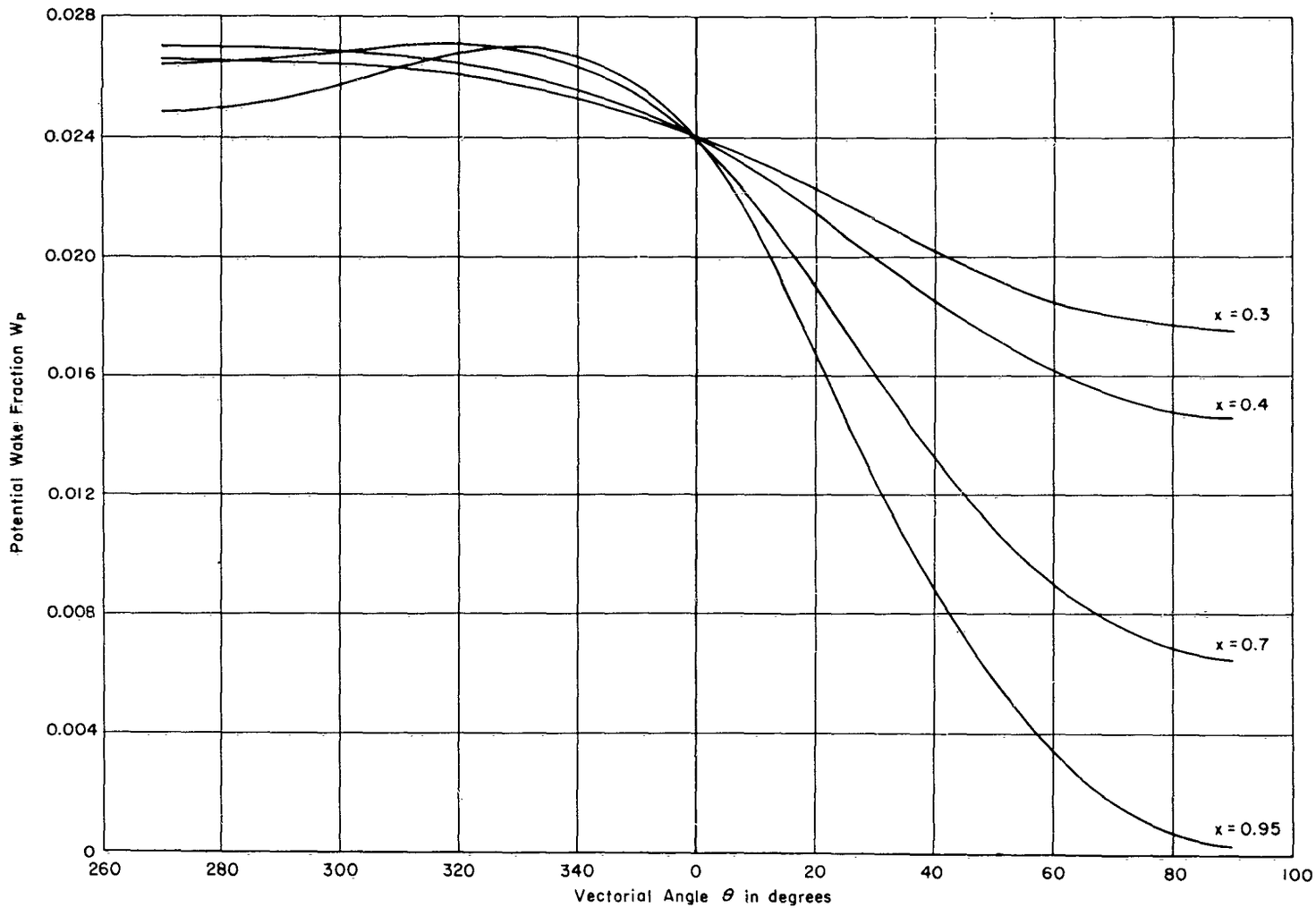

Figure 17c – $\xi = 0.3$

Figure 18 – Computed Potential Wake Fraction, Foil 16-309, $C_L = 0.3$, $\alpha = 0.92$ Degrees, $\xi = 0.15$

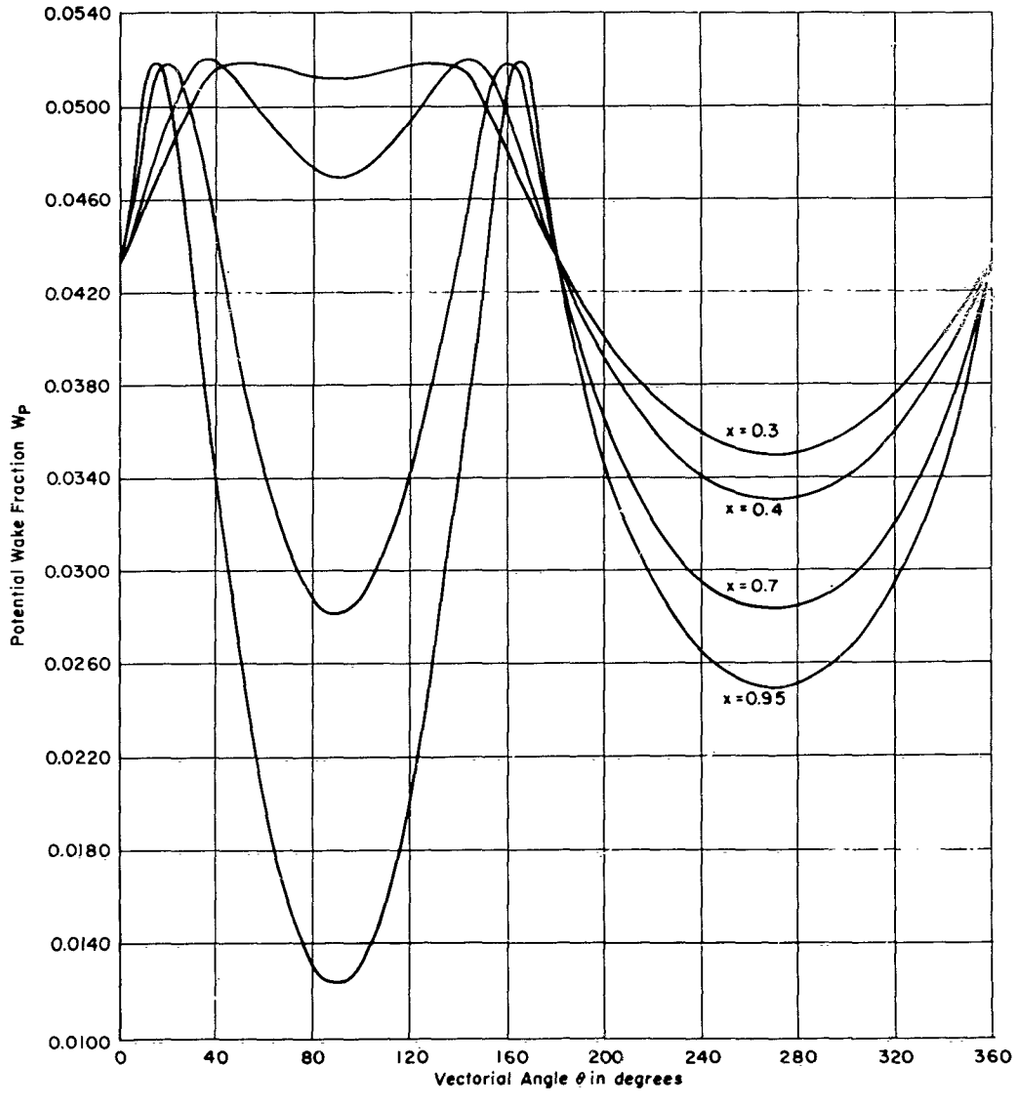

Figure 18a – Foil Off Axis at $0.4R$ in Lift Direction

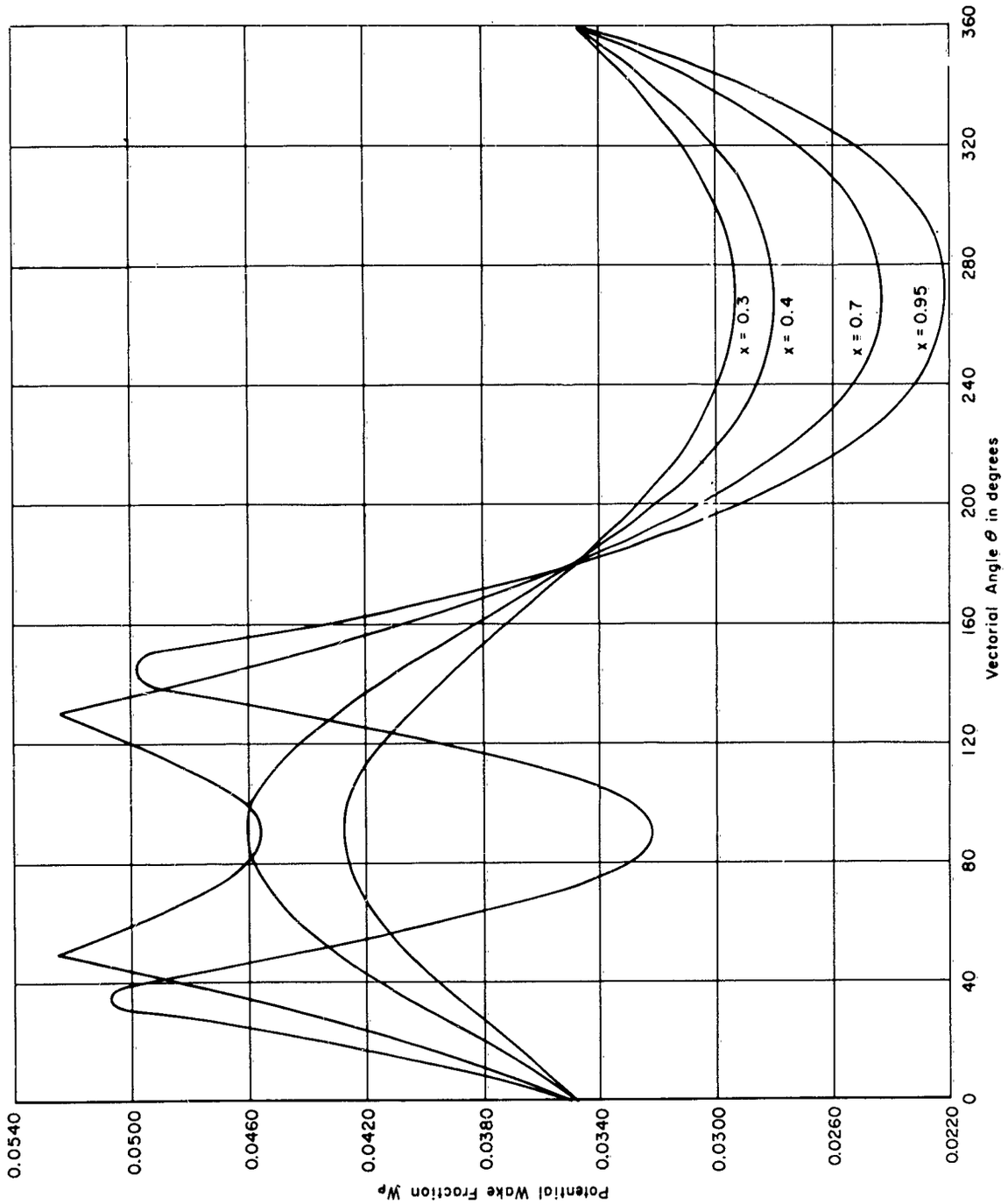

Figure 18b — Foil Off Axis at 0.7R in Lift Direction

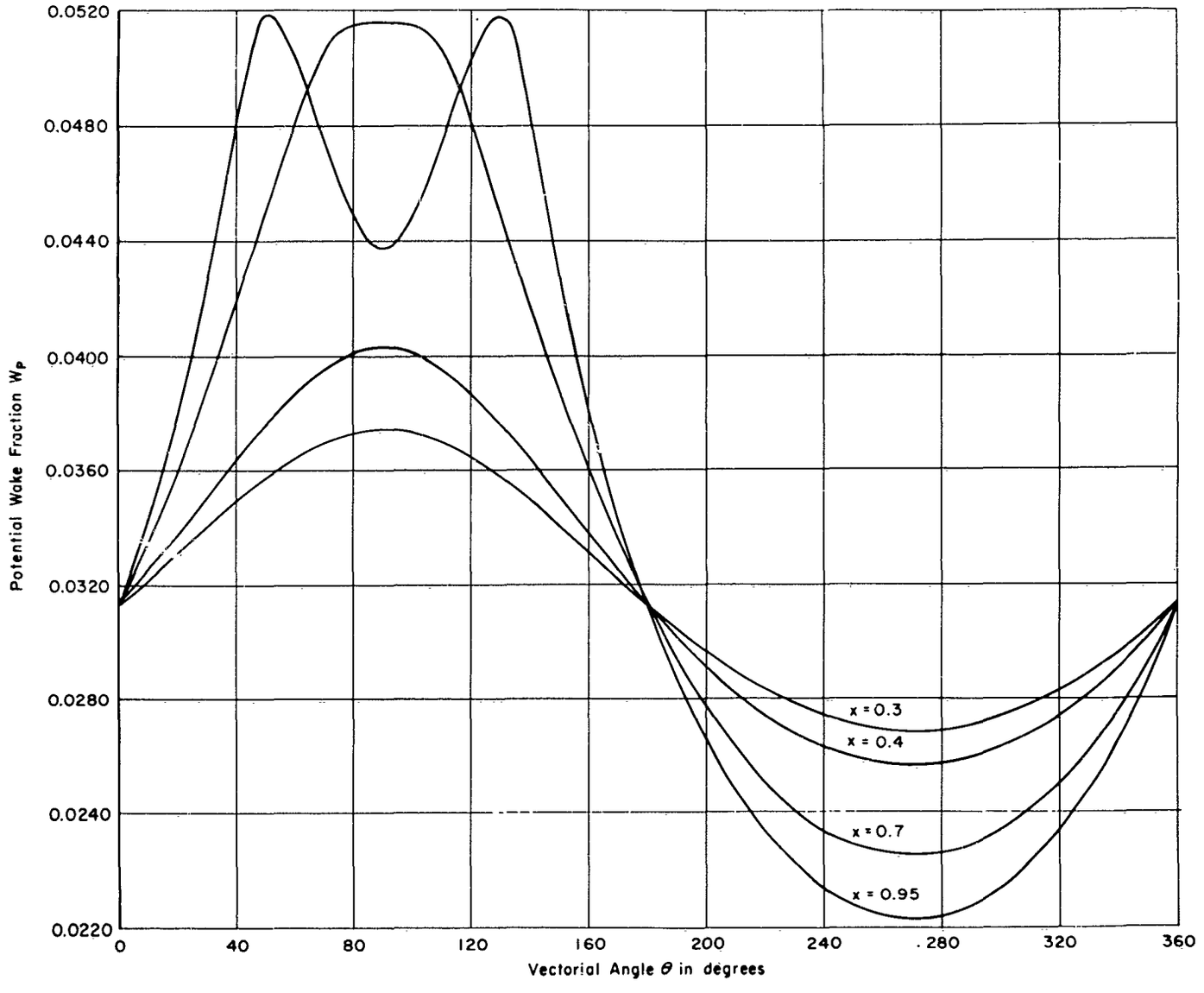

Figure 18c — Foil Off Axis at 0.9R in Lift Direction

APPENDIX B

TEST RESULTS

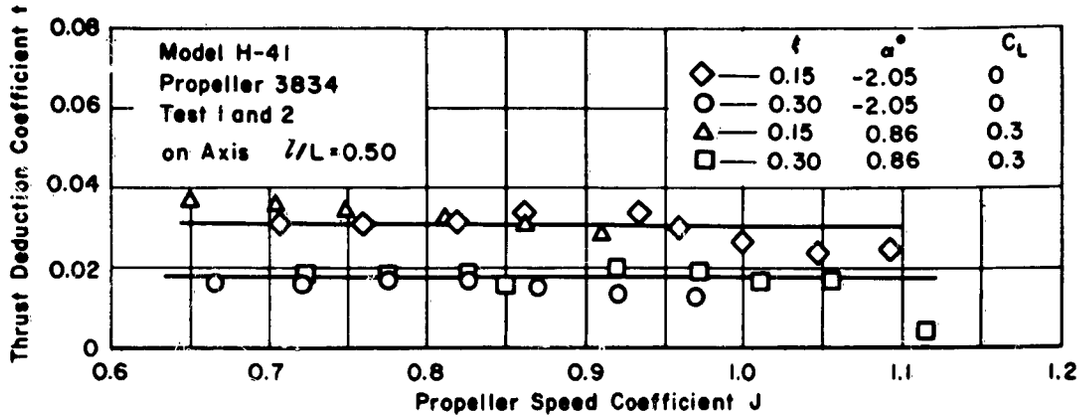

Figure 19 – Thrust-Deduction Coefficient versus Propeller-Speed Coefficient with ξ and C_L as Parameters for Foil without Nacelle, Tests 1 and 2

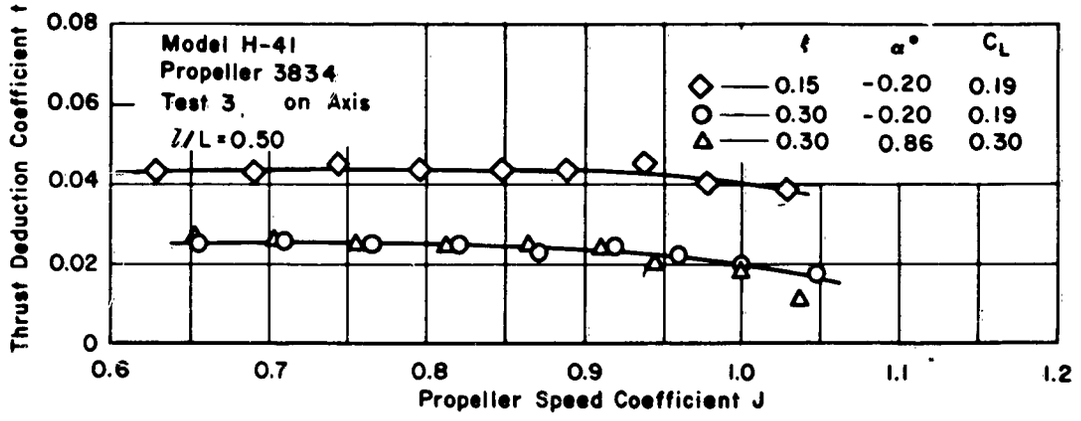

Figure 20 – Thrust-Deduction Coefficient versus Propeller-Speed Coefficient with ξ and C_L as Parameters for Foil with Nacelle, Test 3

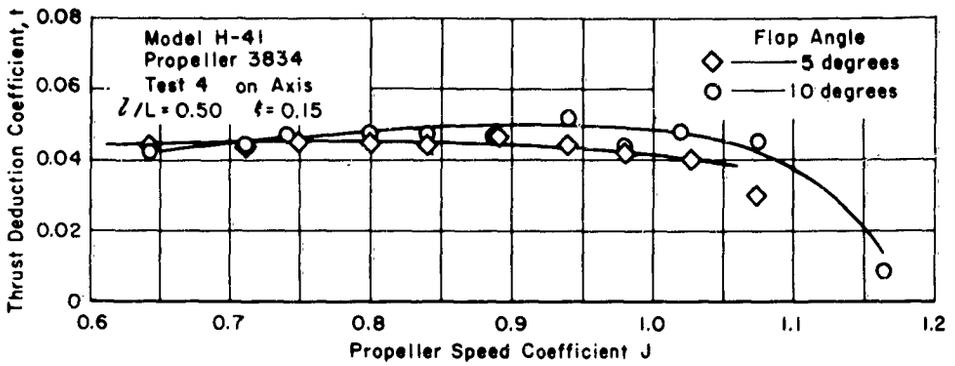

Figure 21 – Thrust-Deduction Coefficient versus Propeller-Speed Coefficient with Flap Angle as a Parameter for Foil with Nacelle, Test 4

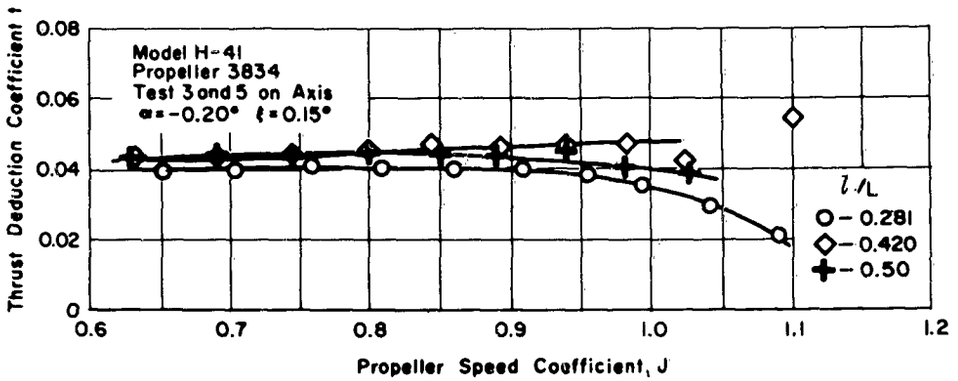

Figure 22 – Thrust-Deduction Coefficient versus Propeller-Speed Coefficient with l/L as a Parameter for Foil with Nacelle, Test 5

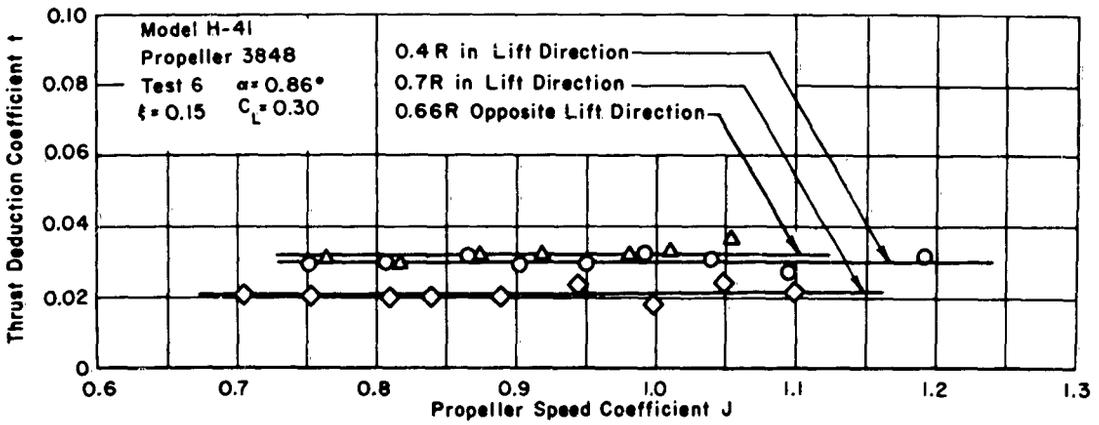

Figure 23 – Thrust-Deduction Coefficient versus Propeller-Speed Coefficient at Off-Axis Positions for Foil without Nacelle, Test 6

REFERENCES

1. Korvin-Kroukovsky, B.V., "Stern Propeller Interaction with a Streamline Body of Revolution," International Shipbuilding Progress, Vol. 3, No. 17 (Jan 1956).

2. Breslin, J.P., "A Simplified Theory for the Thrust Deduction Force on a Body of Revolution," Proceedings Fifth Midwestern Conference on Fluid Mechanics (1957).

3. Astrup, N.C., "A Set of Propellers in Open Water and behind a Body of Revolution," Parts 1 and 2, Norwegian Ship Model Experiment Tank Publication No. 45 and No. 46 (1957).

4. Hickling, R., "Propellers in the Wake of an Axisymmetric Body," Institution of Naval Architects, Quarterly Transactions, Vol. 99, No. 4, (Oct 1957).

5. Weinblum, G., "The Thrust Deduction," American Society of Naval Engineers, Vol. 63 (1951).

6. Beveridge, J.L., "Effect of Axial Position of Propeller on the Propulsion Characteristics of a Submerged Body of Revolution," David Taylor Model Basin Report 1456 (in preparation).

7. Tsakonas, S., "Analytical Expressions for Thrust Deduction and Wake Fraction for Potential Flows," Stevens Institute of Technology, ETT Report 717 (1957).

8. Silverstein, A., et al, "Downwash and Wake behind Plain and Flapped Airfoils," National Advisory Committee for Aeronautics Report No. 651 (1939).

9. Silverstein, A. and Katzoff, S., "Design Charts for Predicting Downwash Angles and Wake Characteristics behind Plain and Flapped Wings," National Advisory Committee for Aeronautics Report No. 648 (1939).

10. Silverstein, A. and Katzoff, S., "A Simplified Method for Determining Wing Profile Drag in Flight," Journal of the Aeronautical Sciences, Vol. 7 (May 1940), pp. 295–301.

11. Burrill, L.C., "Calculation of Marine Propeller Performance Characteristics," Transactions North East Coast Institute of Engineers and Shipbuilders, Vol. 60 (1943–44).

12. Yeh, H.Y., "Thrust and Torque Fluctuations for APA 249, TMB Model 4414," TMB Report 1364 (Jan 1960).

13. Stack, J., "Tests of Airfoils Designed to Delay the Compressibility Burble," National Advisory Committee for Aeronautics Report No. 763 (1943).

14. Scarborough, J.B., "Numerical Mathematical Analysis," 4th Ed., Baltimore, Johns Hopkins Press (1958).

INITIAL DISTRIBUTION

Copies	
9	CHBUSHIPS 3 Tech Info Br (Code 335) 1 Lab Mgt (Code 320) 2 Prelim Des Br (Code 420) 1 Mach, Sci, & Res Sec (Code 436) 1 Sub Br (Code 525) 1 Prop, Shaft & Bear Br (Code 644)
5	CHBUWEPS 2 Tech Libr (Code DL1-3) 1 Fluid Mech & Flight Dyn Br (Code RRRE-7) 1 Supporting Res Br (Code RUAW-42) 1 RUTO-32 Attn: Mr. H. Eggers
3	CHONR 1 Fluid Dyn Br (Code 438) 1 Struc Mech Br (Code 439) 1 Undersea Programs (Code 466)
1	CDR, USNOL
1	DIR, USNRL
1	DIR, USNEES
1	CDR, USNOTS, Pasadena
1	DTMB High-Speed Phenomena Div Langley Field
1	SUPT USNAVPGSCOL
1	NAVSHIPYD PTSMH
1	NAVSHIPYD MARE
1	O in C, USN Sub School Attn: Sub Dept
1	O in C, PGSCOL, Webb
1	DIR, Aero Res, NASA
10	CDR, ASTIA
1	Dir Def R & E
1	Hydro Lab, CIT
2	Dept NAME, MIT
1	DIR, St. Anthony Falls Hydrau Lab

Copies	
1	DIR, ORL Attn: Dr. G.F. Wislicenus
1	DIR, DL, SIT
2	Iowa Inst of Hydrau Res State Univ of Iowa 1 Dr. Hunter Rouse 1 Dr. L. Landweber
1	Dept NAME, Univ of Michigan Attn: Prof R.B. Couch
1	Univ of Notre Dame Attn: Dr. A.G. Strandhagen
3	School of Engin Univ of California 1 Prof H.A. Schade 1 Dept of Naval Arch 1 Engr Libr
1	Oceanics, Inc., Attn: Dr. Paul Kaplan, Pres
1	TRG
1	Hydronautics, Inc.
1	Ingalls Shipbldg Corp., Pascagoula
1	New York Shipbldg Corp., Camden
2	Gen Dyn Corp., EB Div, Groton
1	Bethlehem Steel Co., Shipbldg Div, Quincy Attn: Mr. Hollinshead DeLuce
2	Gibbs & Cox, Inc.
1	NNSB & DD CO., Engin Tech Div Attn: Mr. John Kane
1	Grumman Aircraft Co
1	Boeing Aircraft Corp
1	SNAME Attn: Capt W.N. Landers
1	Douglas Aircraft Co., Inc. Aircraft Div., Long Beach Attn: Mr. John L. Hess

David Taylor Model Basin. Report 1603.
THRUST DEDUCTION DUE TO A PROPELLER BEHIND A HYDROFOIL, by John L. Beveridge. Oct 1962. vi, 37p. illus., graphs, diagrs., tables, refs. UNCLASSIFIED

A method which is based on Lagally's theorem is presented for computing the resistance augmentation, or thrust deduction, for submerged hydrofoil-propeller arrangements. The effect on the magnitude of thrust deduction of foil lift, propeller load, foil span, foil flap angle, and propeller-foil spacing was investigated. Computed examples and experimental thrust-deduction results for several hypothetical arrangements showed good agreement.

1. Hydrofoil-propeller configurations--Thrust deduction--Theory
2. Propulsion--Interaction--Theory
3. Hydrofoil boats--Design
4. Propellers--Thrust fluctuation--Mathematical analysis
5. Nonuniform wake--Mathematical analysis

I. Beveridge, John L.
II. S-R009 01 01

David Taylor Model Basin. Report 1603.
THRUST DEDUCTION DUE TO A PROPELLER BEHIND A HYDROFOIL, by John L. Beveridge. Oct 1962. vi, 37p. illus., graphs, diagrs., tables, refs. UNCLASSIFIED

A method which is based on Lagally's theorem is presented for computing the resistance augmentation, or thrust deduction, for submerged hydrofoil-propeller arrangements. The effect on the magnitude of thrust deduction of foil lift, propeller load, foil span, foil flap angle, and propeller-foil spacing was investigated. Computed examples and experimental thrust-deduction results for several hypothetical arrangements showed good agreement.

1. Hydrofoil-propeller configurations--Thrust deduction--Theory
2. Propulsion--Interaction--Theory
3. Hydrofoil boats--Design
4. Propellers--Thrust fluctuation--Mathematical analysis
5. Nonuniform wake--Mathematical analysis

I. Beveridge, John L.
II. S-R009 01 01

David Taylor Model Basin. Report 1603.
THRUST DEDUCTION DUE TO A PROPELLER BEHIND A HYDROFOIL, by John L. Beveridge. Oct 1962. vi, 37p. illus., graphs, diagrs., tables, refs. UNCLASSIFIED

A method which is based on Lagally's theorem is presented for computing the resistance augmentation, or thrust deduction, for submerged hydrofoil-propeller arrangements. The effect on the magnitude of thrust deduction of foil lift, propeller load, foil span, foil flap angle, and propeller-foil spacing was investigated. Computed examples and experimental thrust-deduction results for several hypothetical arrangements showed good agreement.

1. Hydrofoil-propeller configurations--Thrust deduction--Theory
2. Propulsion--Interaction--Theory
3. Hydrofoil boats--Design
4. Propellers--Thrust fluctuation--Mathematical analysis
5. Nonuniform wake--Mathematical analysis

I. Beveridge, John L.
II. S-R009 01 01

David Taylor Model Basin. Report 1603.
THRUST DEDUCTION DUE TO A PROPELLER BEHIND A HYDROFOIL, by John L. Beveridge. Oct 1962. vi, 37p. illus., graphs, diagrs., tables, refs. UNCLASSIFIED

A method which is based on Lagally's theorem is presented for computing the resistance augmentation, or thrust deduction, for submerged hydrofoil-propeller arrangements. The effect on the magnitude of thrust deduction of foil lift, propeller load, foil span, foil flap angle, and propeller-foil spacing was investigated. Computed examples and experimental thrust-deduction results for several hypothetical arrangements showed good agreement.

1. Hydrofoil-propeller configurations--Thrust deduction--Theory
2. Propulsion--Interaction--Theory
3. Hydrofoil boats--Design
4. Propellers--Thrust fluctuation--Mathematical analysis
5. Nonuniform wake--Mathematical analysis

I. Beveridge, John L.
II. S-R009 01 01